Microtearing modes in core and edge of Tokamaks and their possible role in plasma transport

R Ganesh
Institute for Plasma Research, Bhat, INDIA

Contributions:

Aditya K Swamy (IPR, India)

S. Brunner, J. Vaclavik, L Villard (CRPP, Lausanne)

Outline

- Background & Motivation
  - Microtearing Modes : Literature and some unanswered questions
- Finite β Gyrokinetics
  - Electromagnetic Gyrokinetic Model
  - 2D Eigenvalue Problem
  - Code : EMGLOGYSTO - Eg. ITG with full electron response
- Properties of collisionless Microtearing Modes
  - Without Trapped Electrons
  - Role of Trapped Electrons
  - Role of Magnetic Shear
- Outlook and Issues

Background - Tearing (1)

- In Vacuum, can a magnetic field pattern "tear" and "reconnect"?

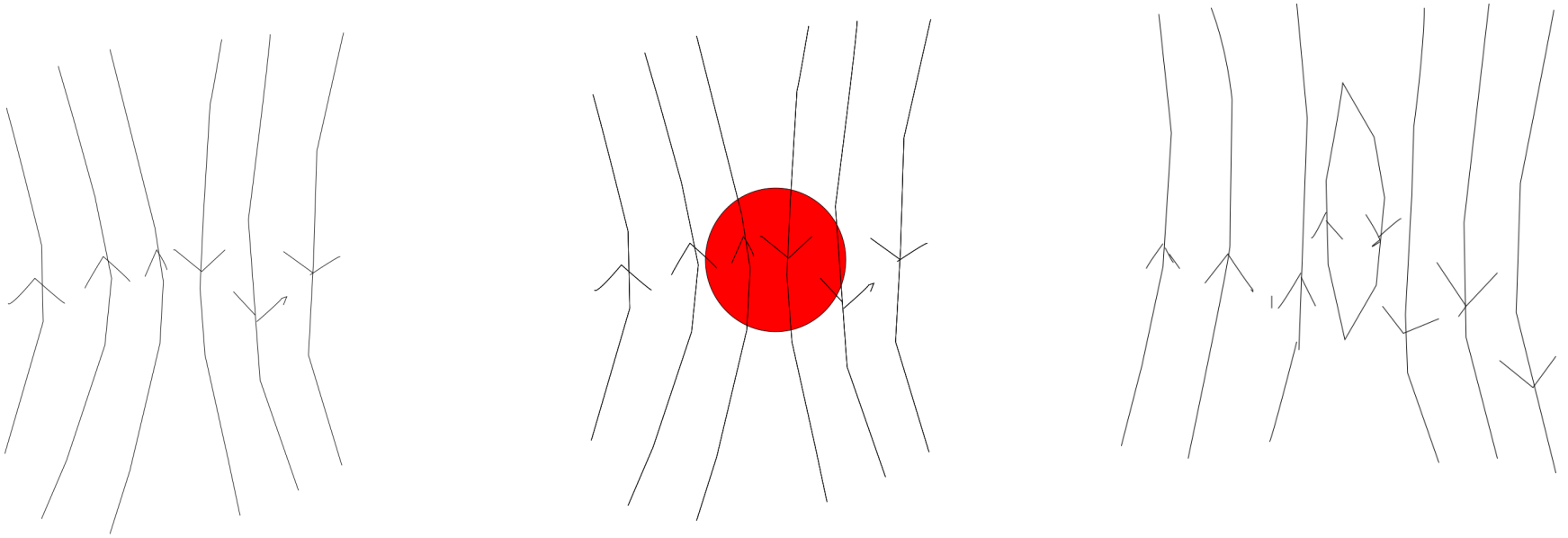

- Difference in Magnetic energy $\delta W = \int \frac{B_{vac}^2 - B_{rec}^2}{2\mu_0}\, dV$ is carried away by plasma particles in the form of current density J
- Current cannot be sustained without some form of effective dissipation α. That is $\vec{E} = \alpha \vec{J}$. Ex. resistivity η such that $\alpha \equiv \eta$ (e-i collisions) and electron inertia $\alpha \propto m_e$ (collisionless)

Background - Tearing (2)

- MHD tearing modes arise due to dissipation
- $\vec{E}_{||}$ necessary to sustain $J_{||}$ - possible only for nonzero dissipation η. $\vec{E} + \vec{V} \times \vec{B} = \eta \vec{J}$ OR $E_{||} = \eta J_{||}$
- $B-$field changes sign around the "tear" or "reconnection region" and is related to $A_{||}$ by space derivative. Hence $A_{||}$ has to be "even" in θ (and r) about a Mode Rational Surface. ($\nabla^2 A_{||} = -\mu_0 J_{||}$)
- Similarly electric potential φ and $A_{||}$ are related through derivative ($E_{||} = -\nabla_{||}\varphi - \frac{\partial A_{||}}{\partial t}$), hence ϕ should be "odd" in θ.
- "Tearing Parity" : $A_{||}$ is "even" in θ, φ is "odd" in θ.
- "Ballooning Parity" : $A_{||}$ is "odd" in θ, φ is"even" in θ.
- MHD Tearing modes stabilize at high toroidal mode number or short scales.

Background - Microtearing Modes

- In an MHD stable hot tokamak plasma, can electron temperature gradient (eTG) in the presence of finite plasma β - drive "Microtearing Modes" unstable at ion gyro length scales?

- Can they exist in all aspect ratio's? Are collisions necessary OR electron inertia would do the job?

- If they exist, MTMs can open up a channel of electron transport? Is the transport then be comparable to ITGs, for example?

- These questions were addressed during mid 70's and mid 80's and MTMs were found to be benign in hot collisionless tokamaks.

Literature - Microtearing Modes (1)

- Hazeltine et al (1975)
  - Slab geometry, eTG can drive tearing instability
  - Parallel thermal force ($\nabla_{||}T$)
  - Collisional dissipation is a must.

- Drake, Lee (1977)
  - Cylindrical geometry
  - 3 collision regimes - Collisionless regime: MTM stable; collisional regime unstable: $\frac{\tilde{B}_r}{B_0} \simeq \frac{a}{L_{Te}}$

- Rechester & Rosenbluth (1978)
  - Island width greater than distance between mode rational surfaces leads to magnetic field stochasticity (Chirikov 1958)
  - $\chi_e^{em} \propto v_{th,e} L_c (\frac{\tilde{B}_r}{B_0})^2$

Literature - Microtearing Modes (2)

- Catto & Rosenbluth (1981)
  - Large aspect ratio
  - Drive: Trapped-passing boundary - electrons crossover with increased collision rate $\rightarrow$ destabilization

- Largely interest in Microtearing modes was subdued for 3 decades

- Renewed interest spurred in 2004 by:
  - Spherical Tokamak (ST) Experiments (high β, large ∇T_e)
  - Possible electron channel of transport in electromagnetic regime
  - Simultaneous physics at electron and ion scales are important
  - Advent of Multiscale, gyrokinetic electromagnetic formalism
  - Computational resources

- Spurred both linear and nonlinear, electromagnetic gyrokinetic simulations in Edge and Core

Literature - Microtearing Modes (3)

- Applegate et al PoP (2004), Roach et al NF (2005)
  - one of earliest works, triggered by MAST Expts

PHYSICS OF PLASMAS VOLUME 11, NUMBER 11 NOVEMBER 2004

Microstability in a "MAST-like" high confinement mode spherical tokamak equilibrium

D. J. Applegate,[a] C. M. Roach,[b] S. C. Cowley,[a] W. D. Dorland,[c] N. Joiner,[a]
R. J. Akers, N. J. Conway, A. R. Field, A. Patel, M. Valovic, and M. J. Walsh[d]
EURATOM/UKAEA Fusion Association, Culham Science Centre, Abingdon, United Kingdom

(Received 24 June 2004; accepted 4 August 2004; published online 18 October 2004)

Gyrokinetic microstability analyses, with and without electromagnetic effects, are presented for a spherical tokamak plasma equilibrium closely resembling that from a high confinement mode (H mode) discharge in the mega-ampere spherical tokamak (MAST) [A. Sykes *et al.*, Nucl. Fusion **41**,

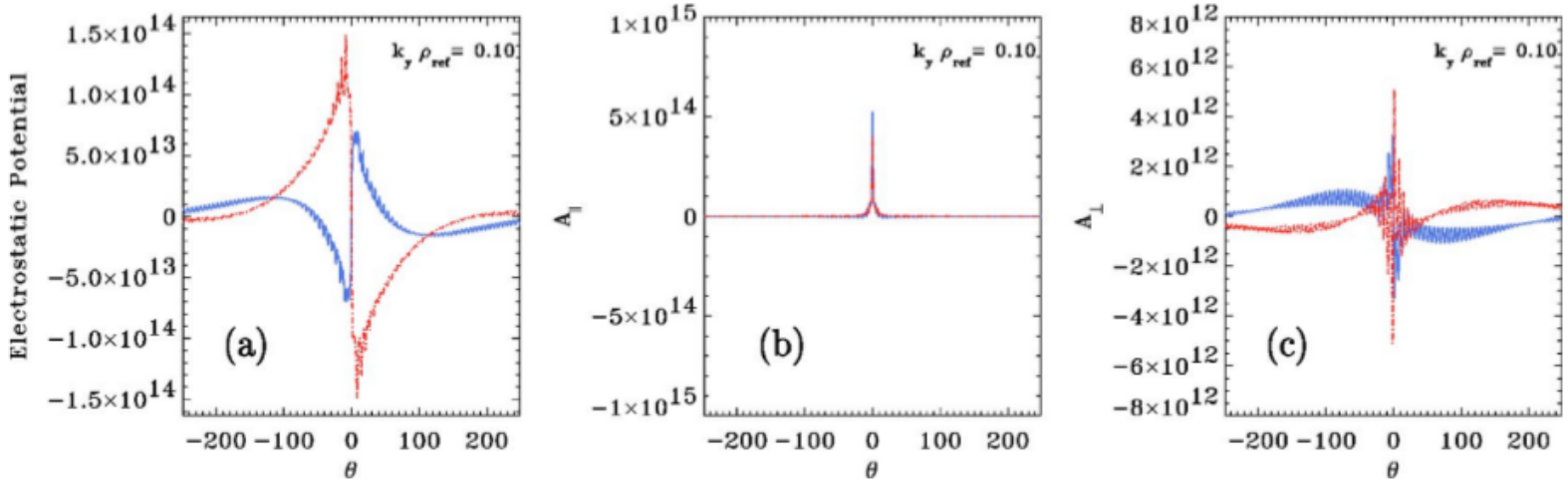

Literature - Microtearing Modes (4)

- Applegate et al PoP (2004), Roach et al NF (2005)
  - For STs, REMOVAL of collisional effects is found to "convert" Microtearing Mode (MTM) to ITG!

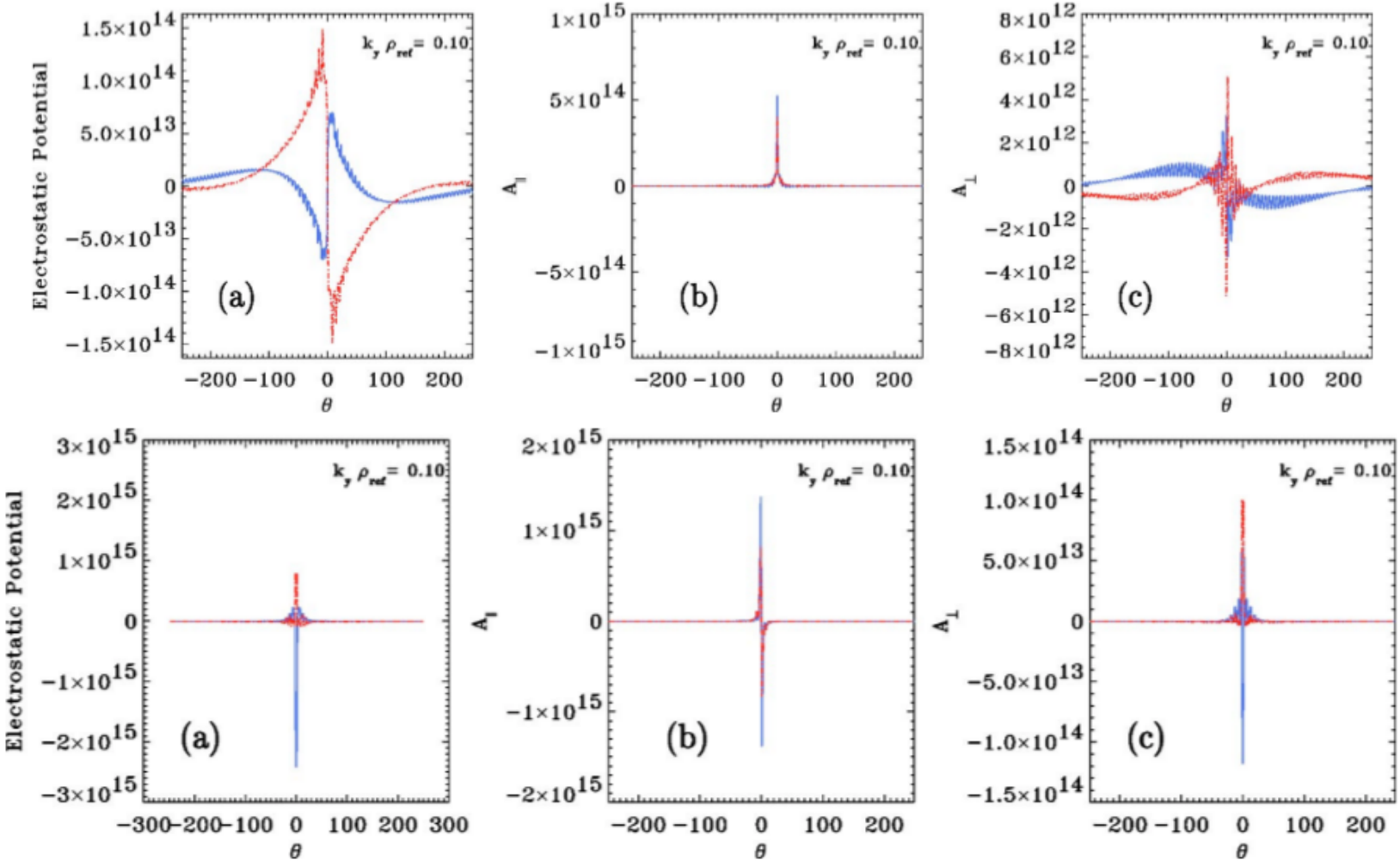

Literature - Microtearing Modes (5)

- Applegate et al PPCF (2007)
  - For STs, Microtearing Mode (MTM) eigenmode structure leading to "torn" $\tilde{J}_{||}$
  - ST Plasma, Aspect Ratio A $\sim$ 1.5, Gyrokinetic, Flux tube (GS2), Collisions (dissipation) necessary, At moderate Aspect Ratio: MTMs unstable and at large Aspect Ratio : weakly unstable - Poincare section starting from mode structure and Hamilton's equation for B-field [Cary et al (1983)].

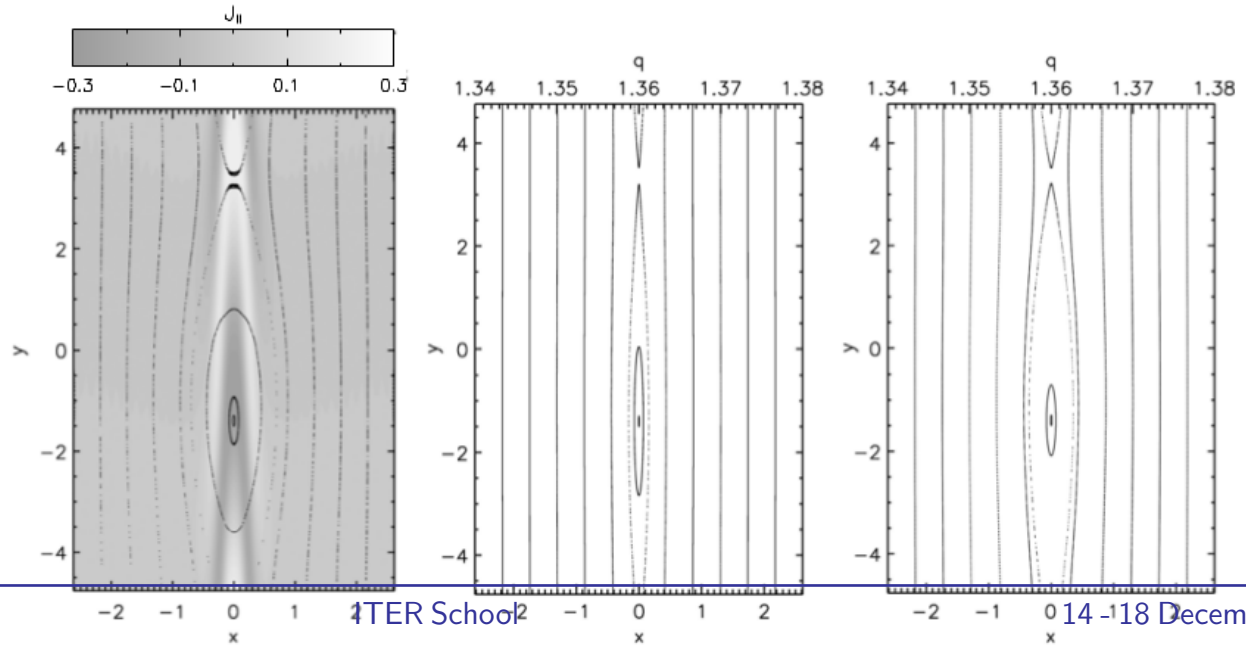

Literature - Microtearing Modes (6)

- Doerk et al PRL (2011), PoP (2012) : Linear results
  - Standard Aspect Ratio Tokamak : Core region
  - Semi-collisional : ν_{ei} using Landau-Boltzmann Operator
  - GENE flux tube, ρ_* scaling $[\rho_* = \frac{\rho_{Li}}{a}]$

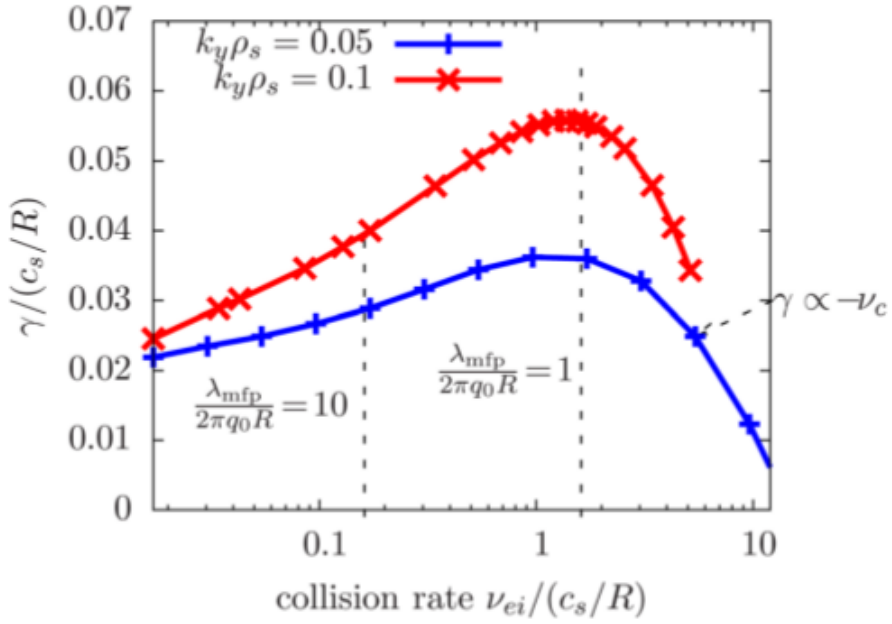

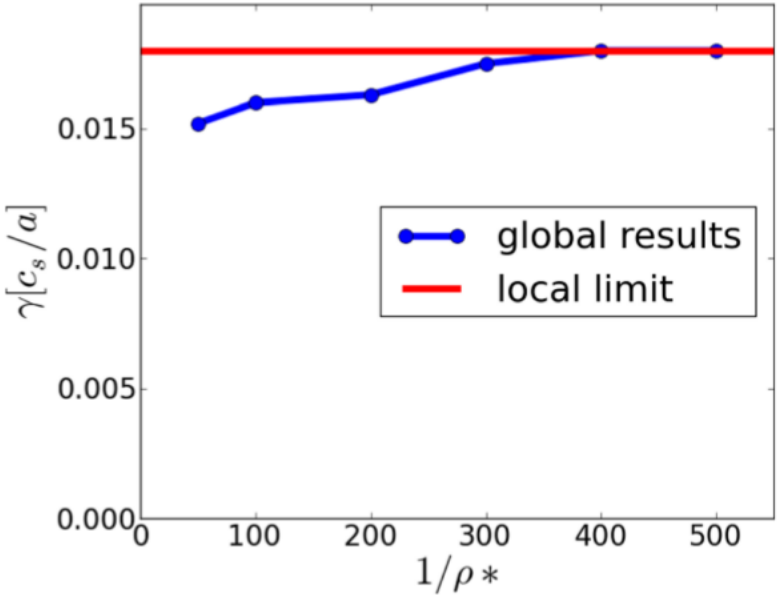

Literature - Microtearing Modes (7)

- Doerk et al PRL (2011), PoP (2012) : Nonlinear, Colls - GENE
- Guttenfelder et al PRL (2011), PoP (2012) : GS2/GYRO Nonlinear studies with collisions
  - Nonlinearity leads to stochasticity of B-field lines and $e-$ transport
  - Strength of "tear field" $\tilde{B}_r$ increases with temperature gradient $\frac{a}{L_{Te}}$ (Drake)
  - Transport at high a/L_{Te} obeys Rechester-Rosenbluth Scaling
  - $\chi_e^{em} \propto v_{th,e} L_c (\frac{\tilde{B}_r}{B_0})^2$

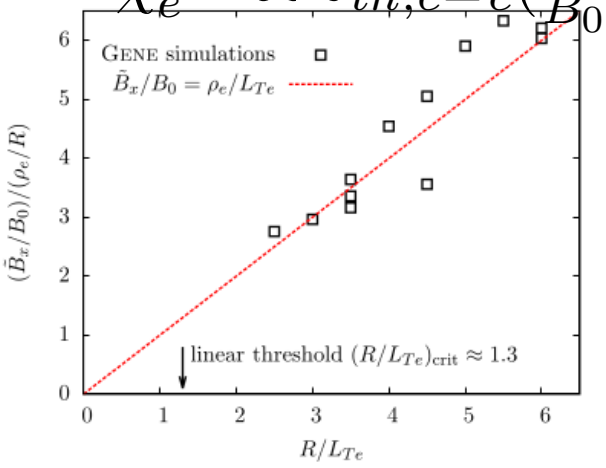

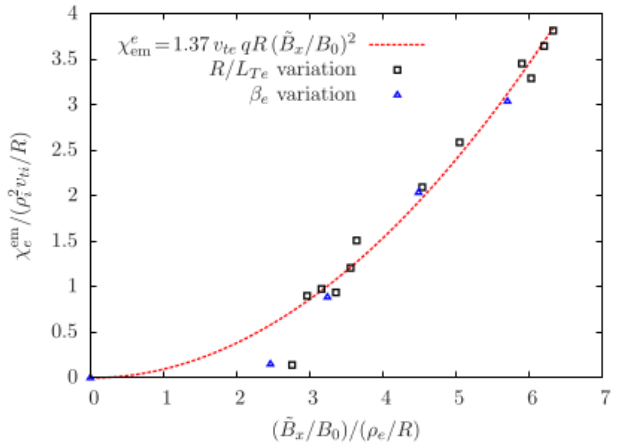

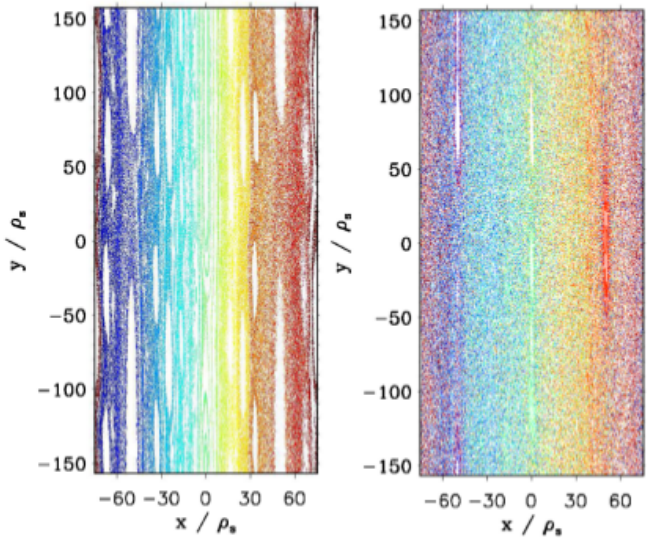

Literature - Microtearing Modes (8)

- Dickinson et al PRL (2012), NF (2013) : linear, Collision - GS2
  - Pedestal : Between two ELMs, what is the pedestal dynamics?
  - In MAST expts, interplay between KBM and MTM?

PRL 108, 135002 (2012) PHYSICAL REVIEW LETTERS week ending 30 MARCH 2012

Kinetic Instabilities that Limit β in the Edge of a Tokamak Plasma: A Picture of an H-Mode Pedestal

D. Dickinson,[1,2] C. M. Roach,[1] S. Saarelma,[1] R. Scannell,[1] A. Kirk,[1] and H. R. Wilson[2]
[1]*EURATOM/CCFE Fusion Association, Culham Science Centre, Abingdon, Oxfordshire, OX14 3DB, United Kingdom*
[2]*York Plasma Institute, Dep't of Physics, University of York, Heslington, York, YO10 5DD, United Kingdom*
(Received 4 October 2011; published 26 March 2012)

Plasma equilibria reconstructed from the Mega-Amp Spherical Tokamak have sufficient resolution to capture plasma evolution during the short period between edge-localized modes (ELMs). Immediately after the ELM, steep gradients in pressure, P, and density, n_e, form pedestals close to the separatrix, and they then expand into the core. Local gyrokinetic analysis over the ELM cycle reveals the dominant

PRL 108, 135002 (2012)

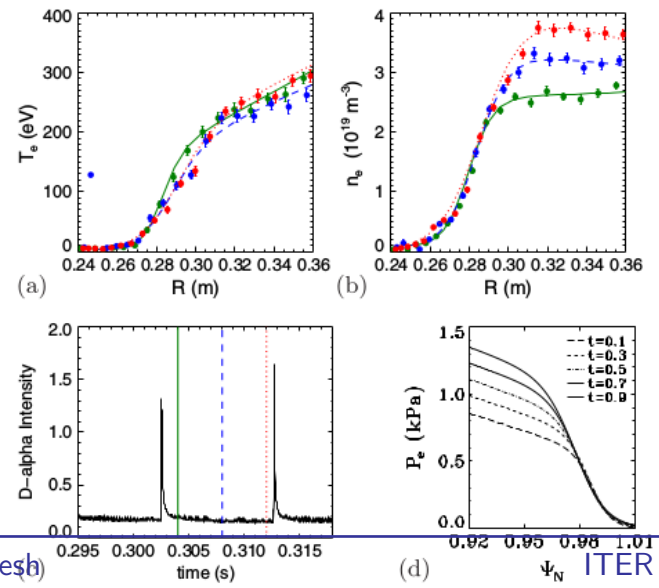

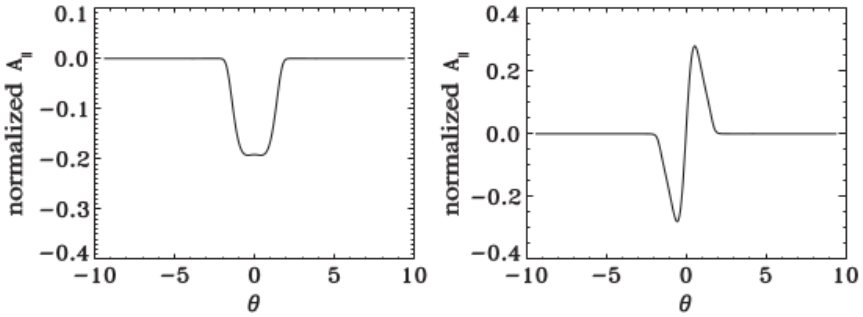

Literature - Microtearing Modes (9)

- Dickensen et al NF (2013)
  - Collisionless MTMs could exist in the edge of STs
  - Destabilizing Mechanism: Magnetic Drift Resonance of Trapped Electrons for all aspect ratio's ϵ
  - Stable collisionless MTMs at large aspect ratio.

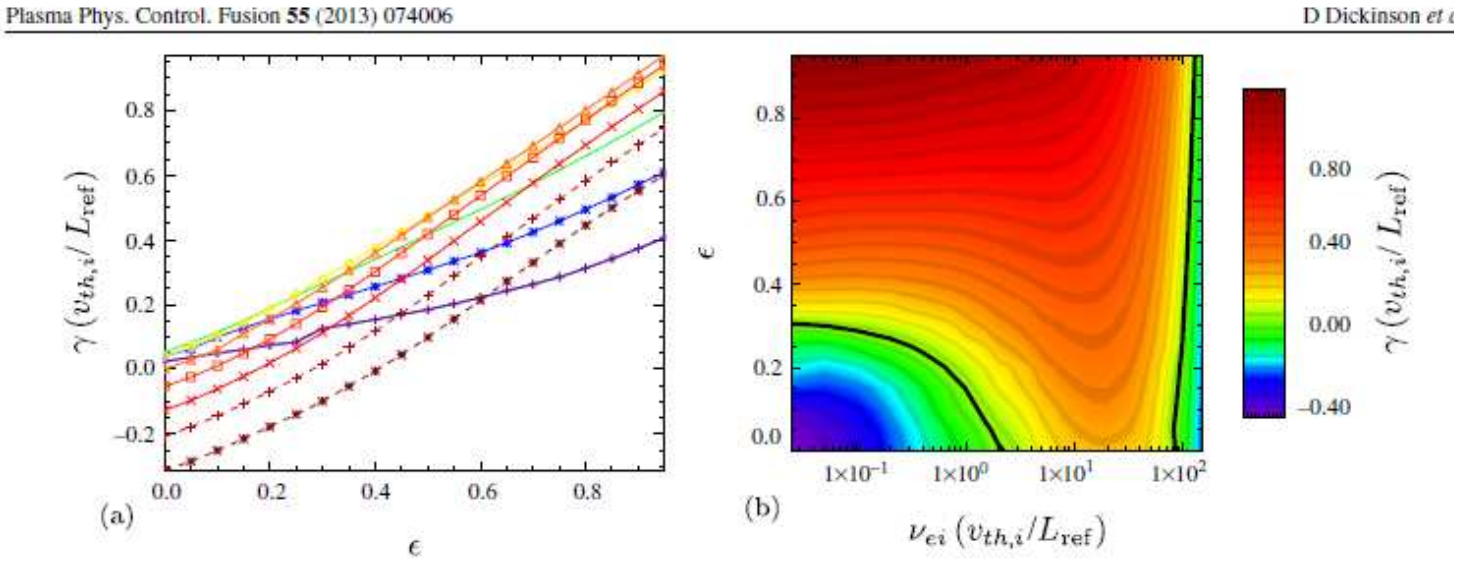

Figure 5. (*a*) $\gamma_{\rm MTM}$ as a function of ϵ for each of the $k_y\rho_i$ values in the key of figure 4 and with $\nu_{ei} = 1.98$. (*b*) $\gamma_{\rm MTM}$ for the dominant $k_y\rho_i = 0.6$ mode as a function of ϵ and ν_{ei}, with —— indicating marginal stability. The frequency, ω, remains between -1.5 and -2.8 throughout these scans.

Literature - So far (10)

- Summary of findings:
  - In slab, straight cylinder and large aspect ratio toroidal geometries, collisions are found to be necessary to drive microtearing modes unstable.
  - Electron temperature gradient in the presence of collisions is the source of free energy.
  - Electrons near passing-trapping boundary in velocity space plus collisions is suggested as another possibility.
  - In Spherical Tokamaks, trapped electrons alone in the presence of high β and strong η_e is found to be important - both in edge/core!
  - In Standard Tokamaks collisions were found to be neccesary, however, results point out existence of unstable collisionless limit.
  - Nonlinear studies in STs and standard Tokamaks in the presence of collisions indicate susbtantial transport due to MTMs

Some important references related MTM not presented here.

- Hazeline, Dobrott, Tsang PoF 1975 - Cylinder, Fokker-Planck, MTM study
- Wang et al, PRL 2007 - Expt and Theory of Collisional Microtearing in NSTX
- Prebedon et al, PRL 2010 - Expt in RFP
- Prebedon et al, PoP 2013 - Expt and simulation in RFP
- D Hatch et al PoP 2013 - Subdominant MTMs in Standard Tokamaks
- Zhin et al, PRL 2013 - Expt in RFP
- AND MORE...

Motivation - Microtearing Modes

- MTMs require fully GK electrons and ions with realistic $\frac{m_i}{m_e}$ and EM:
  - Can unstable collisionless MTMs exist in the core/edge of Large Aspect Ratio (LAR), hot Tokamaks?
  - As the relative fraction of trapped electrons are small in LAR devices compared to STs, can trapped electrons alone be really effective in destabilizing MTMs in LAR devices?
  - Can one stay away from "passing-trapping" boundary and consider only highly passing electrons/ions?
  - What is the role of passing electrons and trapped electrons in destabilizing MTMs in LAR, hot Tokamaks?
  - Would reverse shear affect these modes? Can one construct 2D Mode structure and address "parity" issues?
  - Starting from collisionless Vlasov-Maxwell system, can one address these problems?

Gyrokinetic theory

- Aim of gyrokinetic theory :
  - To describe effectively short perp. wavelength effects in tokamak, keeping FLR information to all orders
  - To efficiently describe low frequency waves (as compared to $\omega_{c,j}$) without resolving in time the Larmor motion
- Small parameters :
  - Ratio of Larmor radius to the Major radius or equilibrium gradient length scale $[\rho_{L,j}/R, \rho_{L,j}/L \ll 1]$
  - Ratio of freq. of plasma disturbance to the gyrofrequency $[\omega/\omega_{c,j} \ll 1]$

Coordinates

- Coordinate system
- Particle types : passing electrons, trapped electrons, passing ions, trapped ions

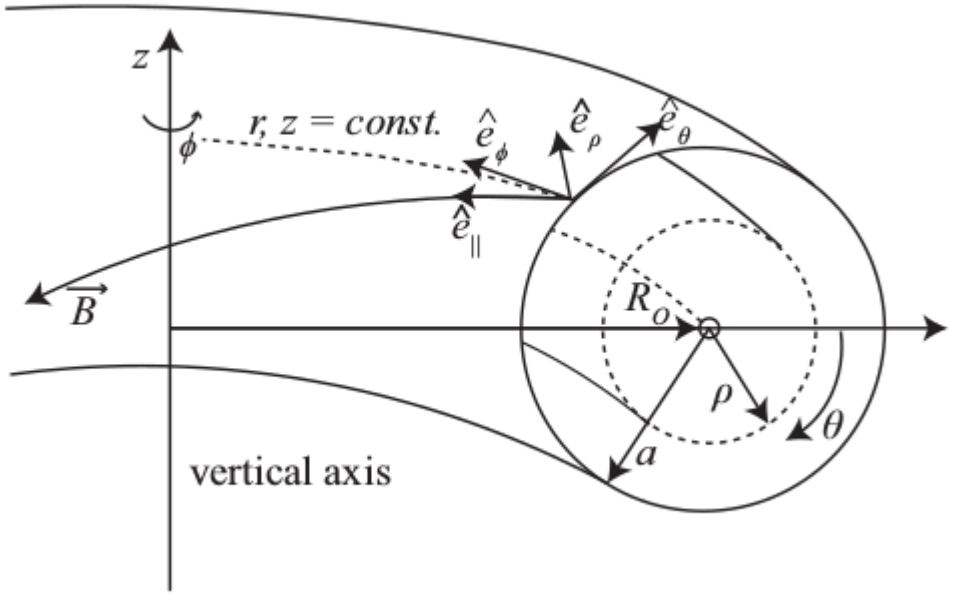

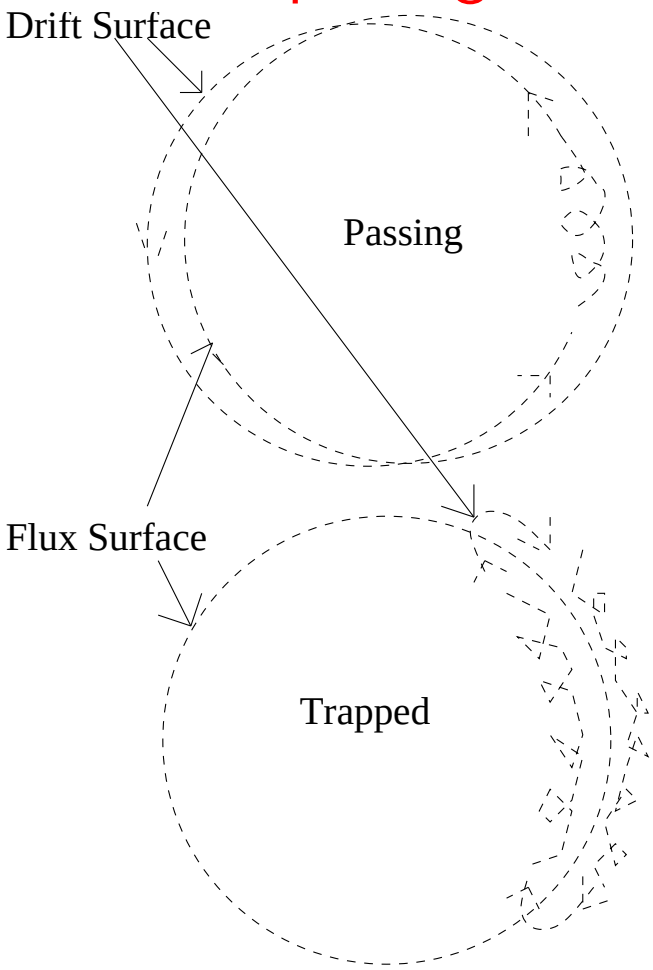

Linearized finite β Gyrokinetics - Basic Steps (1)

- Starting point - Collisionless Electromagnetic Nonlinear Vlasov Maxwell Eqns
- Express in terms of total energy ε, "adiabatic invariant" μ and canonical momentum per particle ψ_p
- Use gyrokinetic ordering $\omega/\omega_{cj} \simeq \mathcal{O}(\rho_{Lj}/L) \ll 1$, $k_{||}/k_{\perp} \simeq \mathcal{O}(\rho_{Lj}/L) \ll 1$
- Linearize for small perturbations around an "equilibrium" f_0
- *Go from real space* $\vec{r} \rightarrow$ *guiding center space* $\vec{R}$ resulting in a "J_0" accounting all order in $k_{\perp}\rho_{Lj}$
- Construct analytically "Greens' Function" $\mathcal{P}_j$ for a "unit source" considering "fully passing ions/electrons" and "fully trapped electrons" perturbatively.

Linearized finite β Gyrokinetics - Basic Steps (2)

- No contribution from particles in the $Passing$-$Trapping\ Boundary$.
- Construct using $\mathcal{P}_j$, the solution to the nonadiabatic response of the distribution for "passing" and "trapped" particles.
- $Get\ back\ to\ real\ space$ which results in additional Bessel Functions
- Get "Closure" using nonadiabatic distribution function by invoking $Quasineutrality$ and $Parallel\ Ampere's\ Law$ (Low β approx).
- Equilibrium gradients in $n_0(r)$ and $T_0(r)$ tend to introduce "convolution" in spectral space resulting in coupling of $\vec{k}$'s
- Results in a Non-Hermitian eigen value problem solved in code EM-$GLOGYSTO$
- Use Nyquist method to solve for eigen values (γ, ω_r). By construction, works only for $\gamma > 0$.

Linear finite β Gyrokinetics - Basic Steps (3)

1. With equilibrium distribution $f_{0j} = f_{0j}(r, v)$ and the perturbed distribution $\tilde{f}_j(r, v, t)$, linearized *gyrokinetic equation* for the non-adiabatic part $h_j(R, v, t)$ is :

$$\left.\frac{D}{Dt}\right|_{u.t.g} h_j(R, v, t) = -\left(\frac{q_j}{m_j}\right)\left[\frac{\partial f_{0j\psi}}{\partial \varepsilon}\frac{\partial}{\partial t} + \frac{v_{||}}{B}\frac{\partial f_{0j\psi}}{\partial \mu}\hat{e}_{||}\cdot\nabla + \frac{1}{\Omega_{pj}}\nabla_n f_{0j}\Big|_{\psi}\hat{e}_{\phi}\cdot\nabla\right]\times$$
$$\left(\tilde{\varphi}(k;)J_0(k_\perp\varrho_j) - v_{||}\tilde{A}_{||}(k;)J_0(k_\perp\varrho_j)\right) + O(\epsilon_g^2) \qquad (1$$

where equilibrium distribution f_{0j} : local Maxwellian

$$f_{0j}(\varepsilon, \mu, \psi) = \frac{N(\psi)}{\left(\frac{2\pi T_j(\psi)}{m_j}\right)^{3/2}}\exp\left(-\frac{\varepsilon}{T_j(\psi)/m_j}\right) \quad [By\ choice\ \partial f_{0j}/\partial\mu \equiv 0]$$

2. Solution to Eq.(1) :

$$h_j(R,v,\omega) = -\left(\frac{q_j F_{Mj}}{T_j}\right)\int dk \exp\left(\iota k\cdot R\right)\left(\omega-\omega_j^*\right)\left(\iota\,\mathcal{P}_j\right)\times \left(\tilde{\varphi}(k)J_0(k_\perp\varrho_j) - v_{||}\tilde{A}_{||}(k)J_0(k_\perp\varrho_j)\right) + O(\epsilon_g^2) \quad (2)$$

where ω_j^* is the *diamagnetic drift frequency* and $\mathcal{P}$ is the "Greens-like function".

3. The unit source solution $\mathcal{P}$ for a given (k,ω) is,

$$\iota\mathcal{P} = \sum_{p,p'}\frac{J_p(\alpha_{mdr}x_{tj}^\sigma)J_{p'}(\alpha_{mdr}x_{tj}^\sigma)}{\omega-\sigma k_{||}v_{||}-p\omega_t}\exp(\iota(p-p')(\theta-\bar{\theta}_\sigma)) \quad (3)$$

where $x_{tj}^\sigma = k_\perp\xi_\sigma$, $\xi_\sigma = v_d/\omega_t$, $v_d = \left(v_\perp^2/2+v_{||}^2\right)/(\omega_c R)$, $\omega_t = \sigma v_{||}/(q(s)R)$, $\sigma = \pm 1$ (sign of $v_{||}$), $k_\perp = \sqrt{\kappa^2+k_\theta^2}$, $k_{||} = [nq(s)-m]/(q(s)R)$ and $\bar{\theta}_\sigma$ is defined as $\tan\bar{\theta}_\sigma = -\kappa/k_\theta$ and $s = r/a$, $a-$ is the minor radius at the plasma edge.

Linear finite β Gyrokinetics - Basic Steps (5)

$$\iota\mathcal{P} = \sum_{p,p'} \frac{J_p(\alpha_{mdr} x_{tj}^{\sigma}) J_{p'}(\alpha_{mdr} x_{tj}^{\sigma})}{\omega - \sigma k_{||} v_{||} - p\omega_t} \exp(\iota(p - p')(\theta - \bar{\theta}_{\sigma})) \tag{4}$$

x_{tj}^{σ} - Magnetic Drift Resonance of Passing Particles leading to radial and polodal coupling

$p\omega_t$ - Resonances of transit frequency and its harmonics

$\sigma k_{||} v_{||}$ - Landau Damping

α_{MDR} - can be varied for "numerical experiments" in the range $[0 - 1]$

4. Closure : Poisson's equation and Ampere's Law in parallel direction to magnetic field.

Linear finite β Gyrokinetics - Basic Steps (6)

- Quasineutrality condition and Ampere law yields the "closure".

$$\sum_j \tilde{n}_j(r;\omega) \simeq 0; \qquad \nabla_\perp^2 \tilde{A}_{||} = -\mu_0 \tilde{J}_{||} \tag{5}$$

- Now, putting back the density/current fluctuations in the quasineutrality/Ampere's law and fourier transforming yields a Convolution Matrix due to equilibrium inhomogeneity.

- $$\sum_{\vec{k}'} \sum_{j=i,e} \mathcal{M}^j_{\vec{k},\vec{k}'} \ [\tilde{\varphi}_{\vec{k}'}, \tilde{A}_{||,\vec{k}'}] = 0$$

  where $\vec{k} = (\kappa, m)$ and $\vec{k}' = (\kappa', m')$. Note that we could have 2 species: passing ions (i), passing electrons (e) or more.

- Also, $\vec{k} = (\kappa, m)$ and $\vec{k}' = (\kappa', m')$. With the following definitions, $\Delta\rho = \rho_u - \rho_l$ (upper and lower radial limits), $\Delta_\kappa = \kappa - \kappa'$ and $\Delta_m = m - m'$ matrix elements are :

Linear finite β Gyrokinetics - Basic Steps (7)

- Matrix elements are :

$$\mathcal{M}^{i}_{\vec{k},\vec{k}'} = \frac{1}{\Delta\rho}\int_{\rho_l}^{\rho_u} d\rho \exp(-\iota\Delta_\kappa\rho) \times \left[\alpha_p\delta_{mm'} + \exp(\iota\Delta_m\bar{\theta})\sum_p \hat{I}^0_{p,i}\right]$$

$$\mathcal{M}^{e}_{\vec{k},\vec{k}'} = \frac{1}{\Delta\rho}\int_{\rho_l}^{\rho_u} d\rho \exp(-\iota\Delta_\kappa\rho) \times \left[\frac{\alpha_p}{\tau(\rho)}\delta_{mm'} + \frac{\exp(\iota\Delta_m\bar{\theta})}{\tau(\rho)}\sum_p \hat{I}^0_{p,e}\right] \quad (6)$$

$$\hat{I}^l_{p,j} = \frac{1}{\sqrt{2\pi}v^3_{th,j}(\rho)}\int_{-vmax_j(\rho)}^{vmax_j(\rho)} v^l_{||}dv_{||}\exp\left(-\frac{v^2_{||}}{v^2_{th,j}(\rho)}\right)\left\{\frac{N^j_1 I^\sigma_{0,j} - N^j_2 I^\sigma_{1,j}}{D^{\sigma,j}_1}\right\}_{p'=p-}$$

- Velocity Space Integrals are:

$$I^\sigma_{n,j} = \int_0^{v_{\perp max,j(\rho)}} v^{2n+1}_\perp dv_\perp \exp\left(-\frac{v^2_\perp}{2v^2_{th,j}(\rho)}\right) J^2_0(x_{Lj}) J_p(x'^\sigma_{tj}) J_{p'}(x'^\sigma_{tj})$$

Linear finite β Gyrokinetics - Basic Steps (8)

- The definitions for Vel. Integrals: $v_{\perp max,j(\rho)} = min(v_{||}/\sqrt{\epsilon}, v_{max,j})$ which is "trapped particle exclusion" from ω independent perpendicular velocity integral $I^{\sigma}_{n,j}$; $\alpha_p = 1 - \sqrt{\epsilon/(1+\epsilon)}$ is the fraction of passing particles; $\hat{I}^{l}_{p,j}$, is $\omega - dependent$ parallel integrals; $x^{\sigma}_{tj} = k_{\perp}\xi_{\sigma}$, $N^{j}_{1} = \omega - w_{n,j}\left[1 + (\eta_j/2)(v^2_{||}/v^2_{th,j}) - 3)\right]$; $N^{j}_{2} = w_{n,j}\eta_j/(2v^2_{th,j})$ and $D^{\sigma,j}_{1} = < w_{t,j}(\rho) > (nq_s - m'(1-p)(\sigma v_{||}/v_{th,j}) - \omega$ where $< w_{t,j}(\rho) > = v_{th,j}(\rho)/(rq_s)$ is the average $transit\ frequency$ of the species j.

- As integrals $I^{\sigma}_{n,j}$ are independent of ω and dependent only on $v_{\perp}$, σ and other equilibrium quantities, one may choose to calculate and store them as interpolation tables (memory intensive) or alternatively, one may choose to calculate them when needed (CPU-time intensive).

- Various numerical convergence tests should be performed with number of radial and poloidal Fourier modes, equilibrium profile discretization and velocity integrals.

- Even in a linear calculation, extensive velocity and real space grid size scaling is a must before one takes the results of the code seriously!. This is specially true for addressing 2D (global), MTMs with GK, EM electrons and ions in collisionless limit!!

Linear finite β Gyrokinetics - Summary (1)

- Linear gyrokinetic eqns is formally solved using the equilibrium trajectories of particles.
- As the drift excursions are of $\mathcal{O}(\rho_{L,j}/R_0)$, a perturbative solution for guiding centre drift yields analytical solution for the Propagators (unit source solution) for both passing and trapped particles (not shown, but the method is the same!)
- This solution depends only on equilibrium quantities!
- Spatial inhomogeneity introduces coupling in spectral space $[\vec{k}]$.
- Model includes fully nonadiabatic ions and electrons - at the same physics footing!. This becomes possible because its a linear, spectral approach in space and time. Electrons and ions are not "pushed" in time as in PIC or Eulerian codes!

Linear finite β Gyrokinetics - Summary (2)

- Particles which are "deeply trapped" or "deeply passing" are treated correctly.
- In this model, physics of particles near the passing-trapping border in vel-space are not included.
- FLR effects to all orders in $k_\perp \rho_{L,j}$ are retained for all species!
- The model in its final form is solved numerically in the code EM-GLOGYSTO.
- Code is MPI/OPENMp based and runs on several nodes. Recently a portable version based on FFTW has been developed.
- CODE IS FREE FOR ANYONE INTERESTED!

Optimization - EMGLOGYSTO

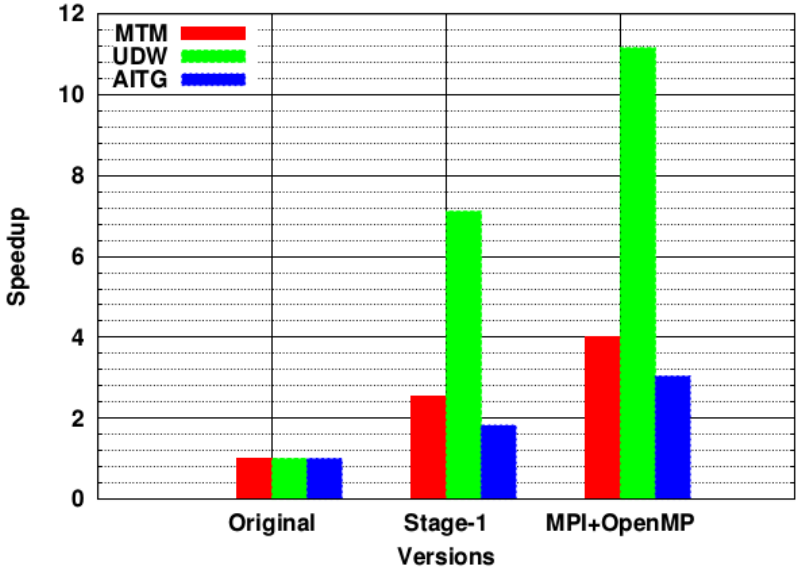

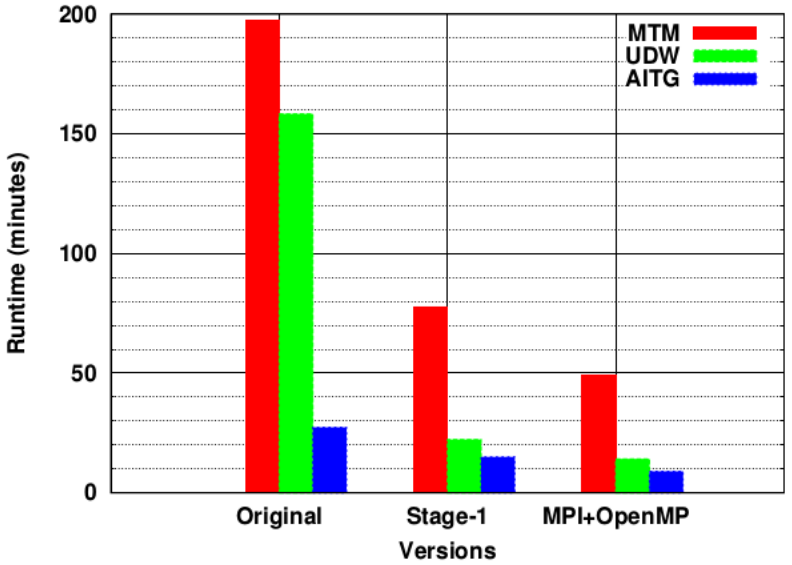

- In principle, "Zero" grid-size dissipation, both in velocity and real space, necessary for addressing "collisionless" physics.
- EM-GLOGYSTO is well optimized for huge velocity space and real space griding.

Linearized finite β Gyrokinetics - Related publications

Related work:

S. Brunner, PhD Thesis (1997) : Propagator, Electrostatics

G. Falchetto, PhD Thesis (2001) : low β Electromagnetics

R. Ganesh et al, PoP (2004), PRL (2005) : high β Electromagnetics

P. Angelino, PhD Thesis, (2006) : Flows

J. Chowdhury, PhD Thesis, (2010) : Electrostatic Instabilities

Aditya K Swamy et al PoP Aug (2014) : This presentation.

Aditya K Swamy et al PoP Sep (2015) : This presentation.

Aditya K Swamy PhD Thesis (2015) : This presentation.

Aditya K Swamy, Shear studies (in Preparation) (2016)

Equilibrium Profiles

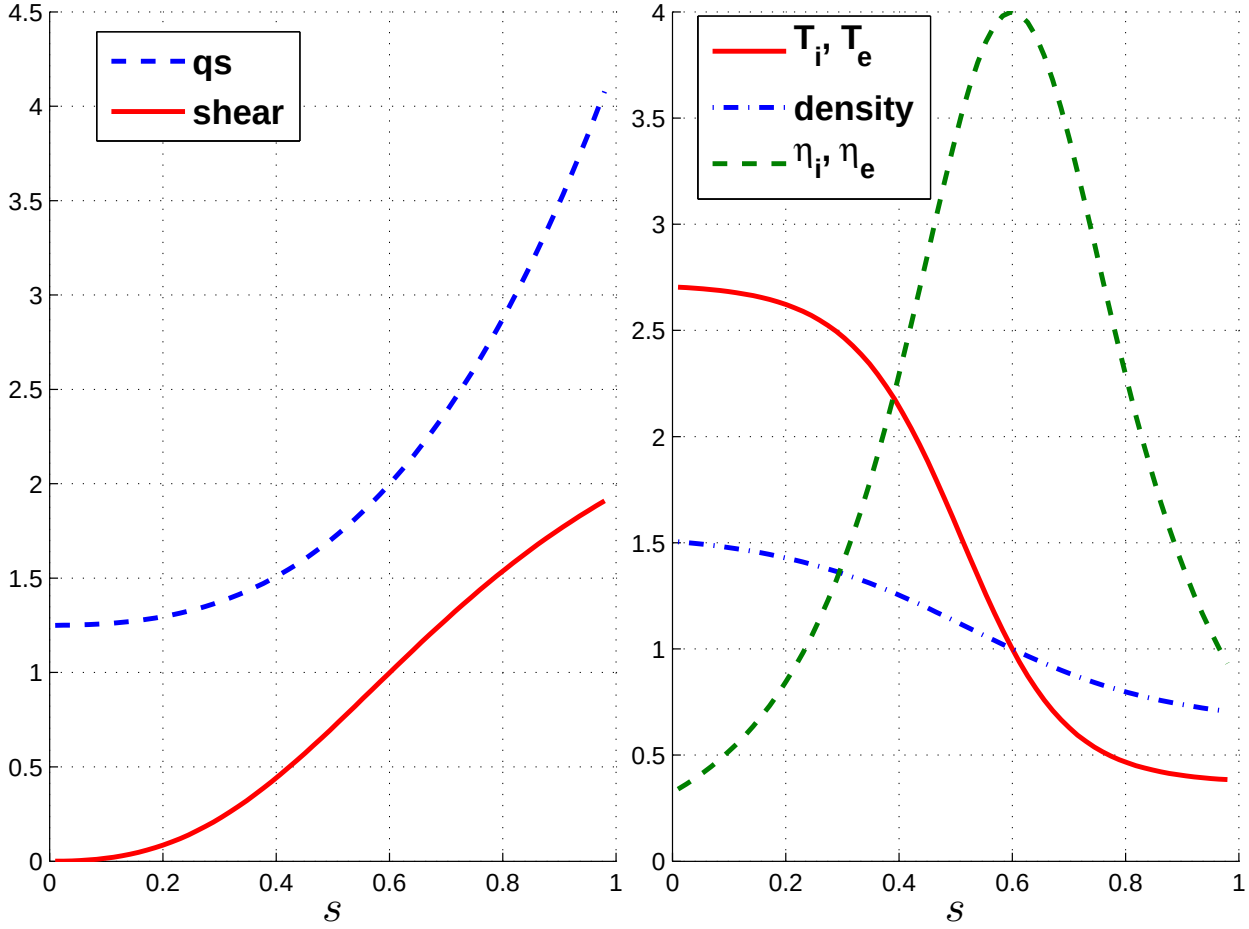

- System size : $R/a = 4.0,\ T_i(s_0) = T_e(s_0) = 7.5\ keV,\ a/\rho_{Li}(s_0) = 57.5$ with $s_0 = 0.6$
- KSTAR ($R/a \simeq 3.6$), EAST ($R/a \simeq 4.0$), SST ($R/a \simeq 4.0$)

Mode rational surfaces - MRS

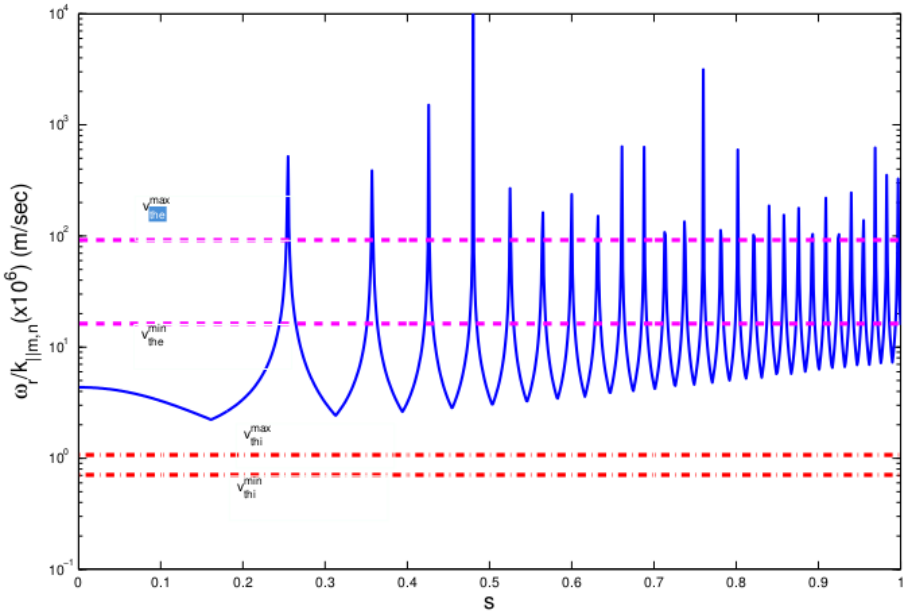

- "Cylindrical" $k_{||}$ is : $k_{||,m,n}(r) = \frac{nq(r)-m}{Rq(r)}$. In a toroidal system, at any "$s = \frac{r}{a}$", m is coupled to $m+1$, $m-1$, $m-2$, $m+2$... Hence toroidal $k_{||}(r)$ is $< k_{||,m,n} >$
- At mode rational surfaces $< k_{||,m,n} > \simeq 0$, thus parallel phase velocity $\frac{\omega_r}{<k_{||,m,n}>}$ can be "large"
- If $\frac{\omega_r}{<k_{||,m,n}>} < v_{th,j}$, species respond "adiabatically" or "spontaneously". If $\frac{\omega_r}{k_{||,m,n}} \geq v_{th,j}$, the species respond "nonadiabatically" or with some "delay"

Global mode structure with spatially varying particle response

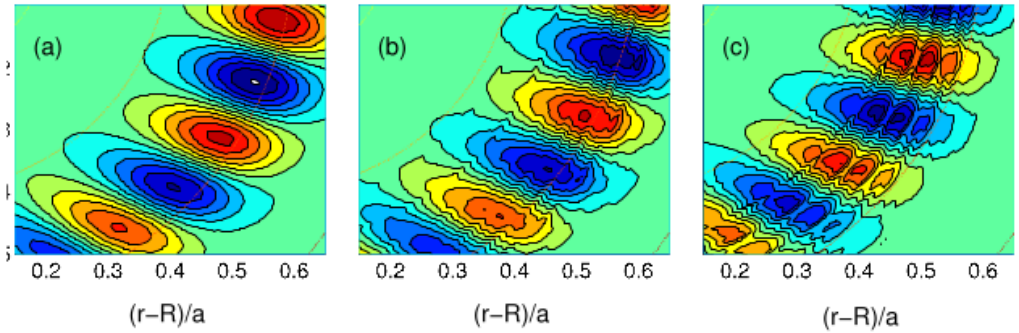

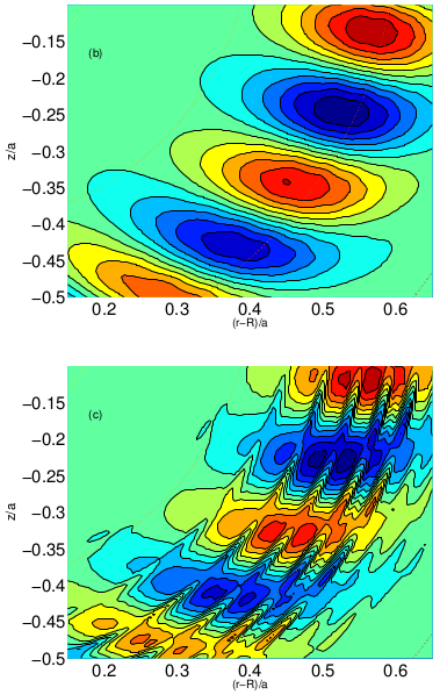

- In a global model, a test for fully nonadiabatic response for electrons and ions is the "structure" around MRSs. For ITG mode, structure (left) is compared with "adiabatic" electron response. Toroidal mode number is $n = 9$ and $\eta_{i,e} = 2, 4$. Same for ITG-TEM (Trapped electrons included).
- An unstable ITG mode structure shows that near MRSs, electron nonadiabaticity brings in sharp radial structure as parallel phase velocity of the mode is large compared to species thermal speed.
- Away from MRSs, electron response is "adiabatic".

PROPERTIES OF MTM : WITHOUT TRAPPED ELECTRONS

Properties : Variation of γ, ω_r with Toroidal mode number n (1)

- For the same equilibrium profiles, growth rate γ (left) and real frequency ω_r (right) are obtained for MicroTearing Mode (Red) and Alfven ITG or KBM (Blue)

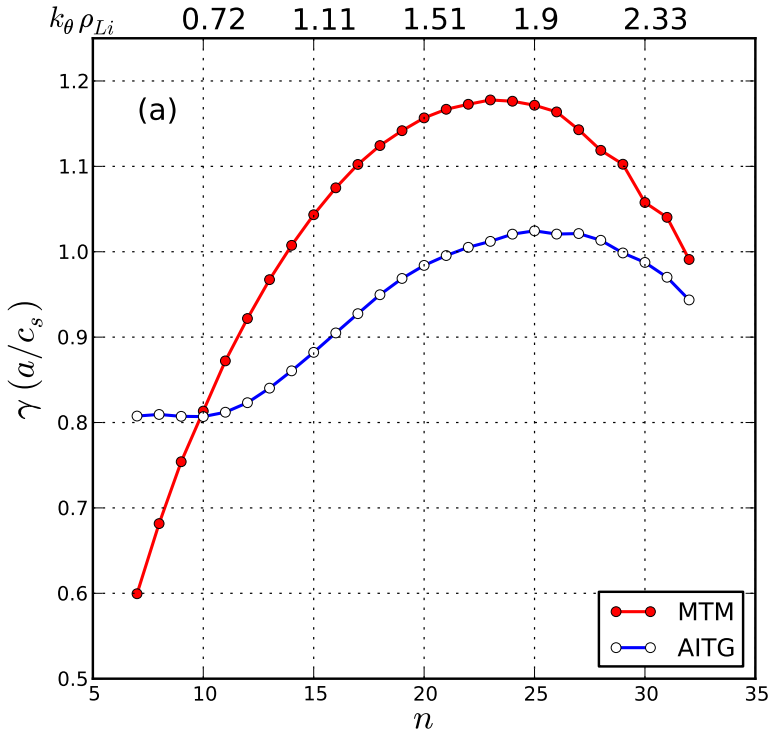

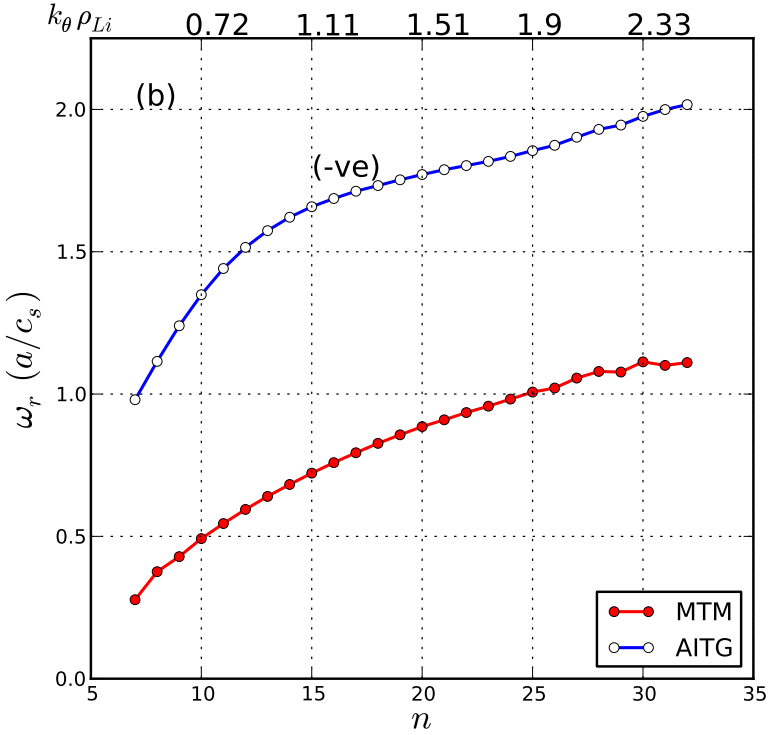

- Fastest growing mode is around $n \simeq 23 - 25$ for both MTM and AITG
- $0.6 \leq k_\theta \rho_{Li} \leq 2.4$ for MTM

Properties : Eigenmode average wavenumbers (2)

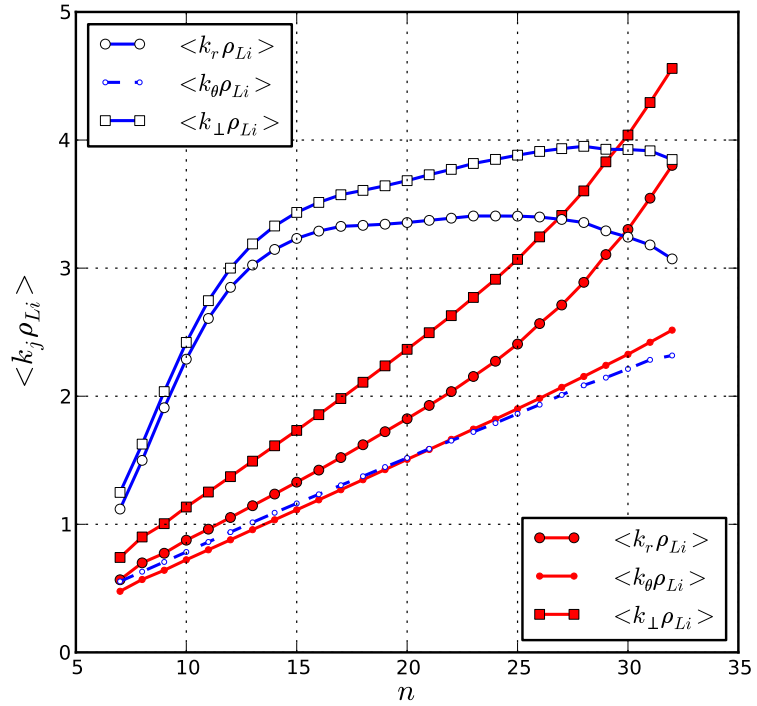

- Due to sharp structures in radial direction, $0.5 \leq < k_r\rho_{Li} > \leq 4$ for MTM

Properties : 2D Eigenmode Structures - Real(φ) (3)

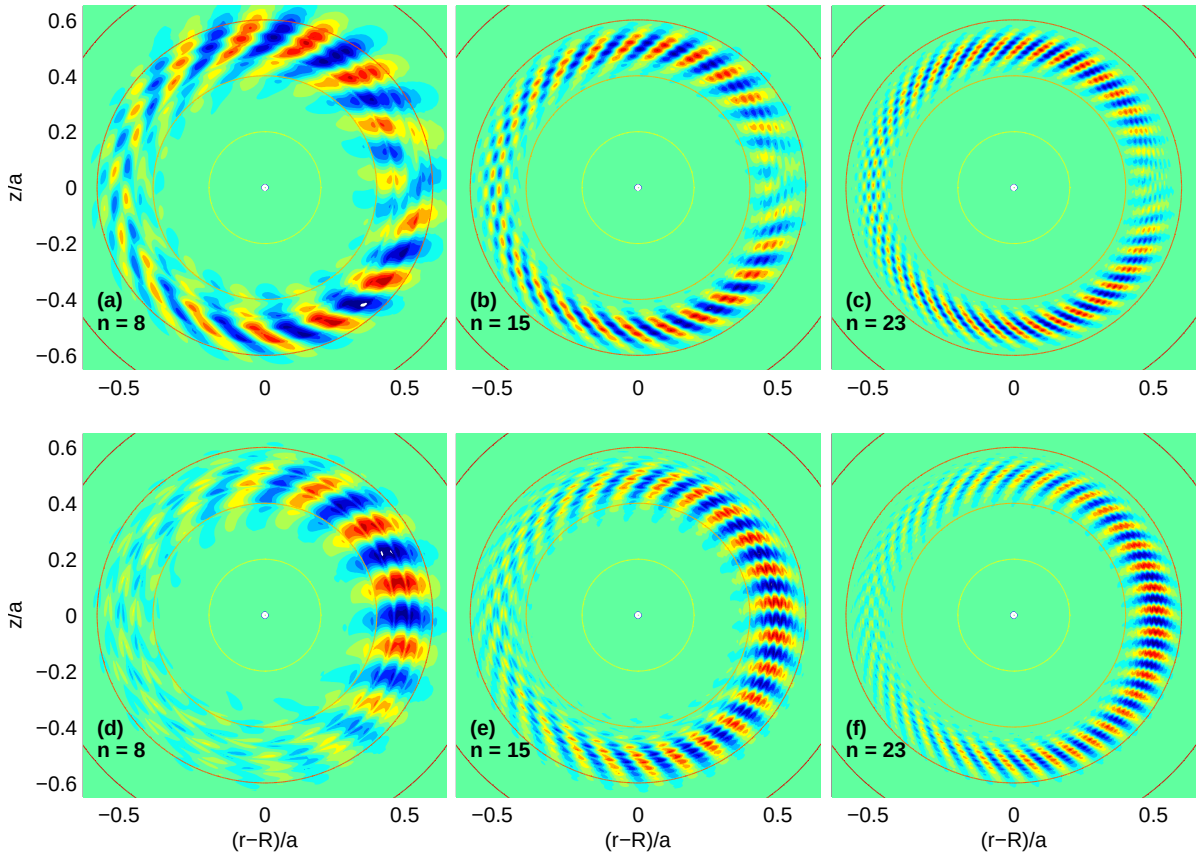

- Re($\varphi(r, \theta)$) is plotted for MTM (top row) and AITG (bottom row) for $n = 8, 15, 23$
- For each radial location, MTM mode φ structure is seen to exihibit "tearing parity" along θ while AITG exihibits "ballooning parity"
- Imaginary part of $\varphi(r, \theta)$ is negative of Real part. Imag(φ) is not shown

Properties : 2D Eigenmode Structures - Real($A_{||}$) (4)

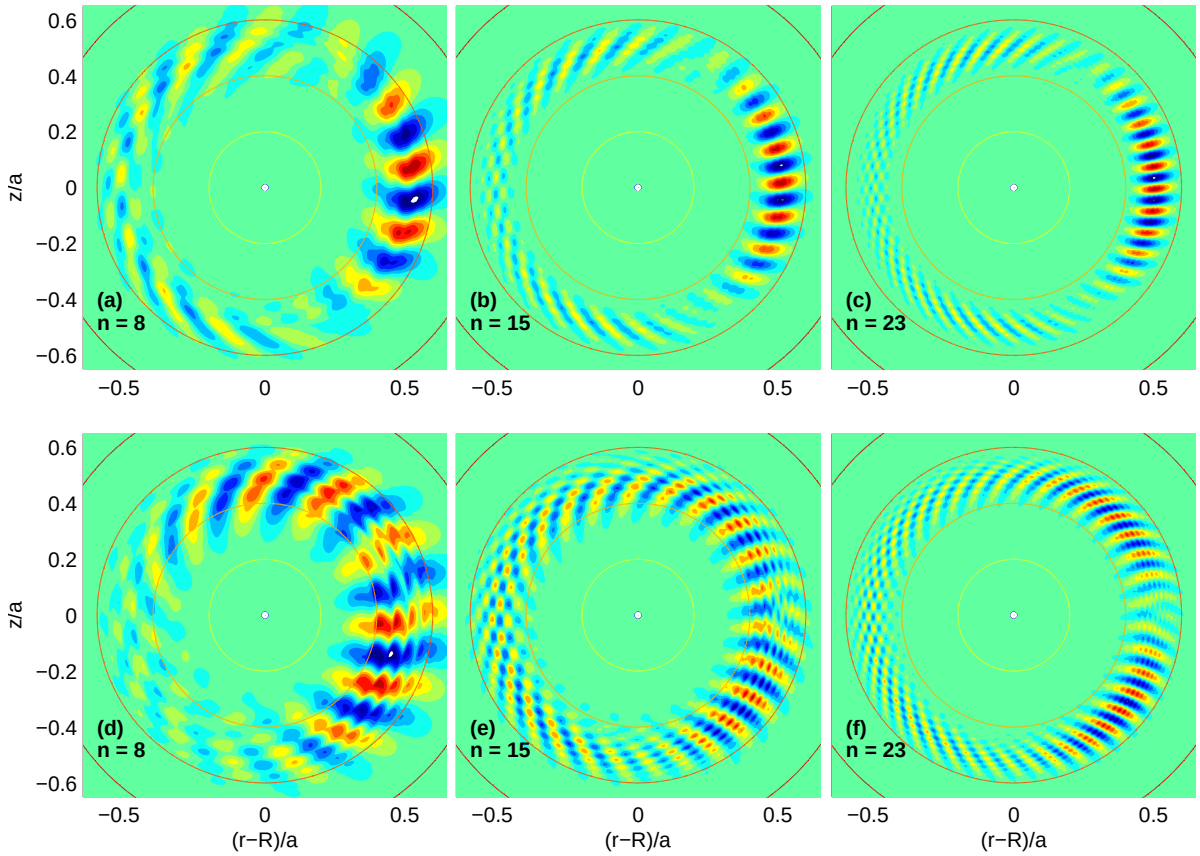

- Re($A_{||}(r,\theta)$) is plotted for MTM (top row) and AITG (bottom row) for $n = 8, 15, 23$
- The symmetries are "swapped" between MTM and AITG.
- Imaginary part of $A_{||}(r,\theta)$ is negative of Real part. Imag($A_{||}$) is not shown

Properties : Radially averaged 1D mode structures (5)

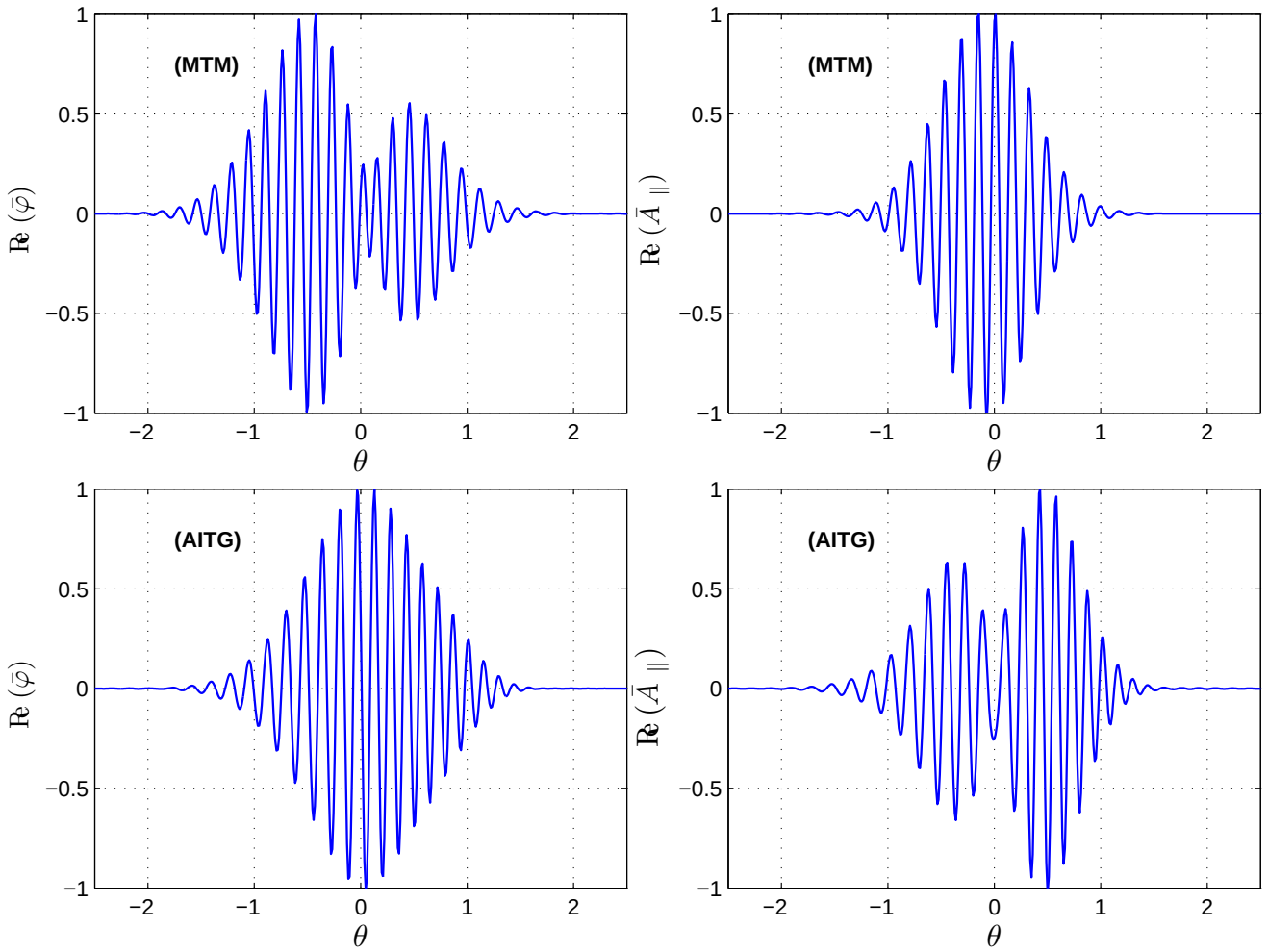

- "Envelope" of $\bar{\varphi}(\theta)$ and $\bar{A}_{||}(\theta)$ exihibit clear "parity swap" for MTM and AITG.

Properties : Poloidal coupling and radial extension of $|\varphi|$ (6)

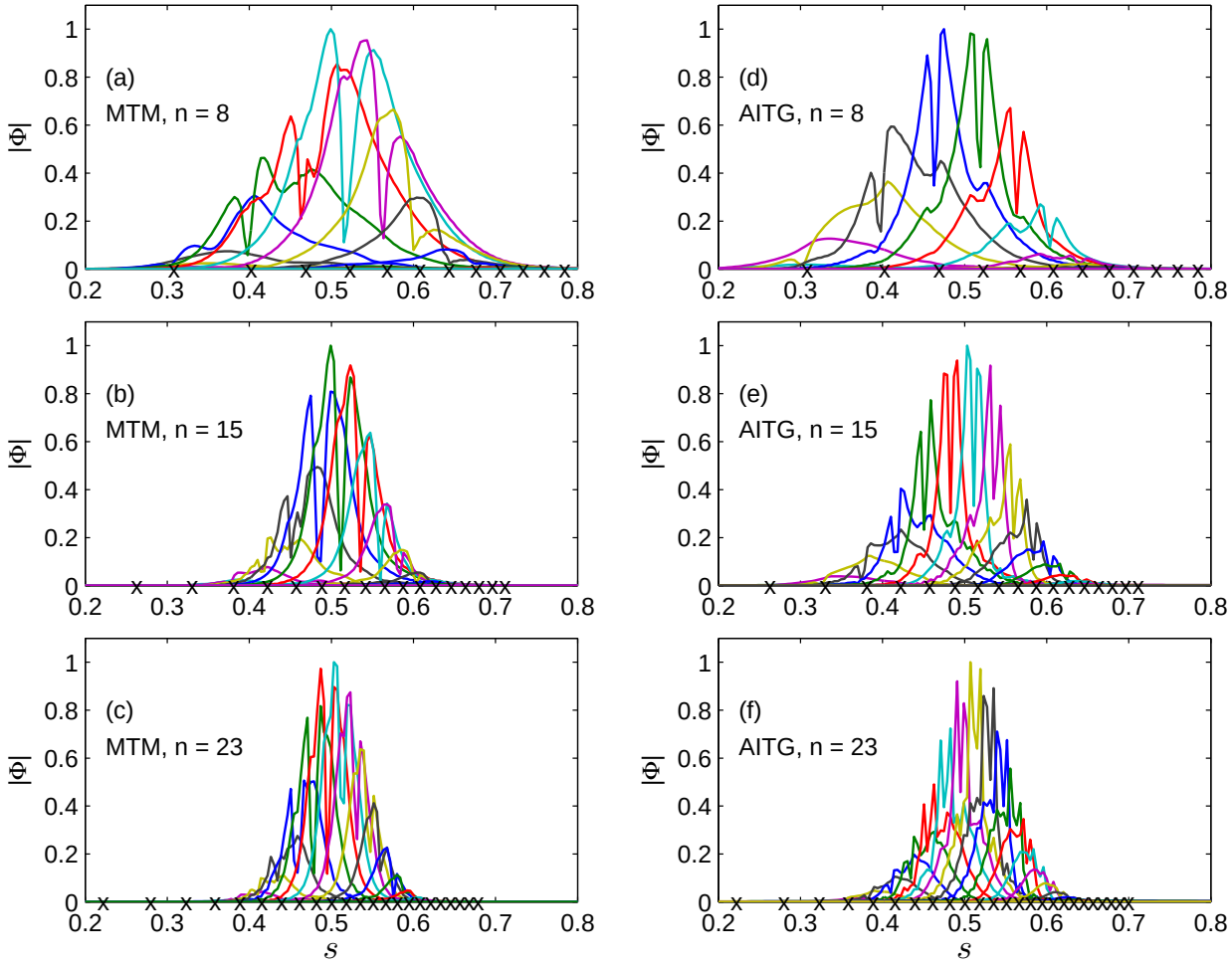

- $|\varphi_m(r)|$ across the minor radius shows that both AITG and MTM are radially extended modes for the equilibrium considered.

- Due to toroidicty induced magnetic drift, a strong poloidal mode coupling is seen. Sharp gradients appear at location where "cylindrical" $k_{m,n} \simeq 0$.

Properties : Poloidal coupling and radial extension of $|A_{||}|$ (7)

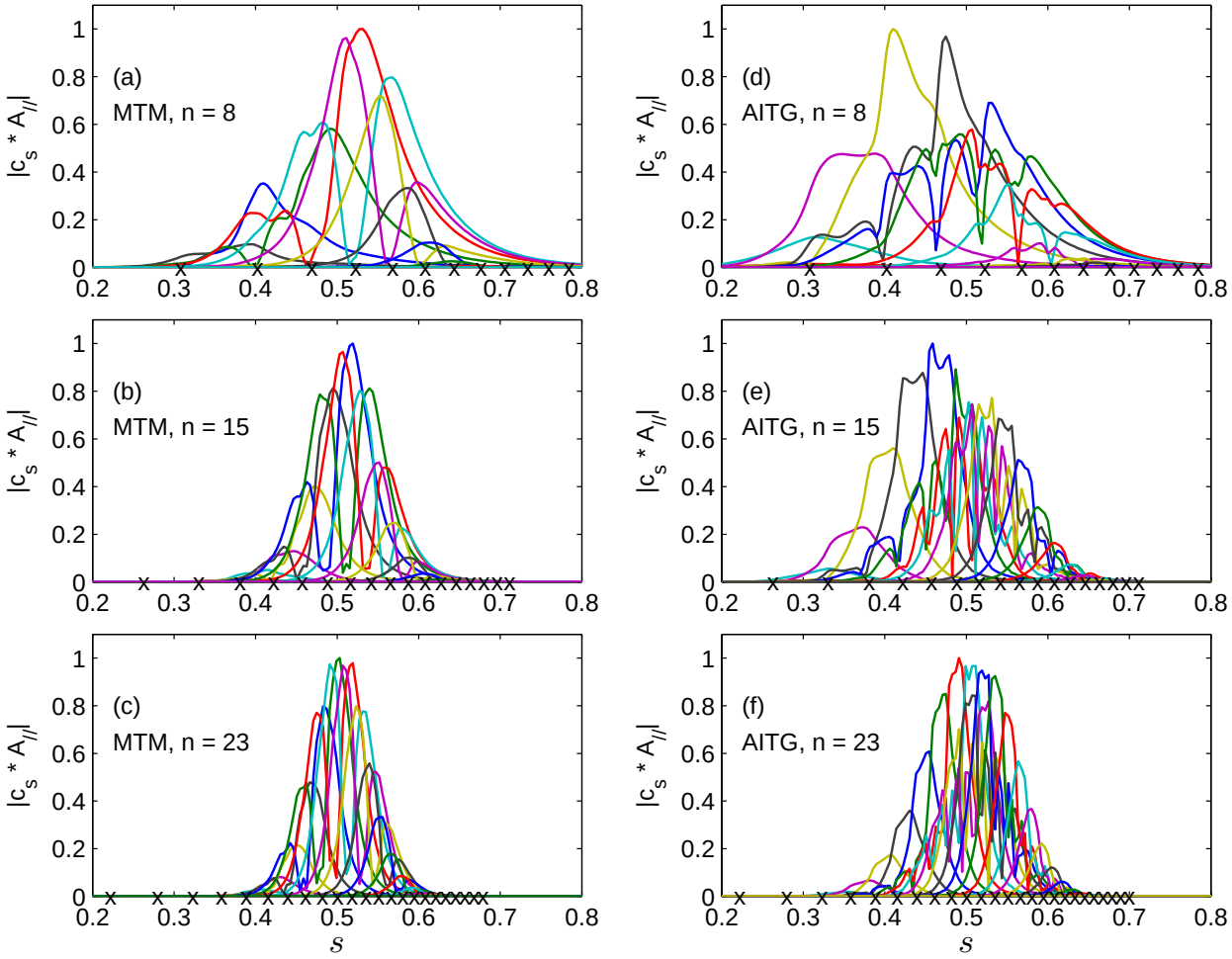

- Variation of $|A_{||,m}(r)|$ across the minor radius.
- Due to toroidicty, a strong poloidal mode coupling is seen. Sharp gradients appear at location where $k_{m,n} = 0$. Mode averaged $< k_{||} > \neq 0$!

Properties : Mode rational surfaces and mode structure : $|\varphi|$ (8)

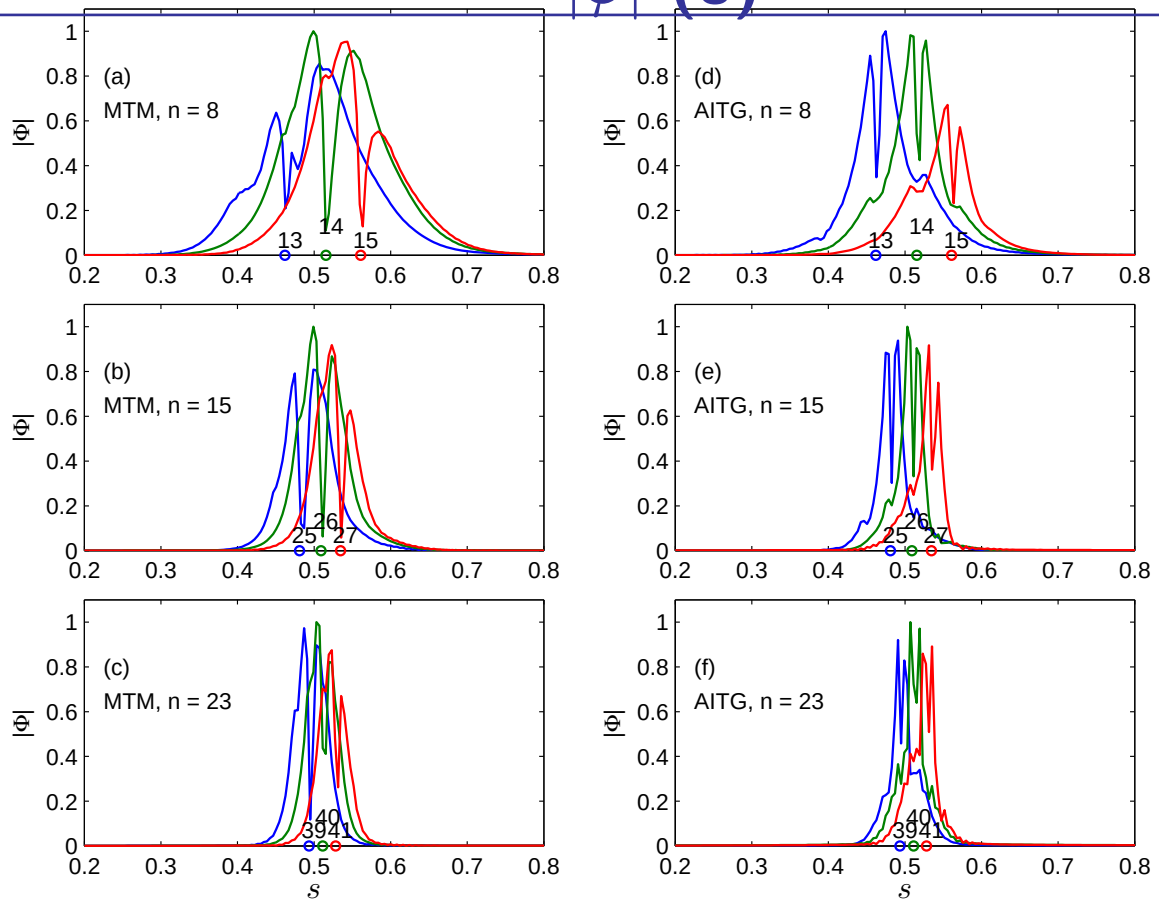

- $|\varphi_m(r)|$: Three polodial modes with largest relative amplitudes is shown for both AITG and MTM. Location of mode rational surface (indicated on the x-axis) exactly coincide with the sharp structures.

- "Cylindrical" phase velocities $\omega_r/k_{||,m,n} \simeq v_{th,e}$. Nonadiabatic effects becomes important. Resulting sharp structures necessitate large radial resolution.

Properties : Mode rational surfaces and mode structure : $|A_{||}|$ (9)

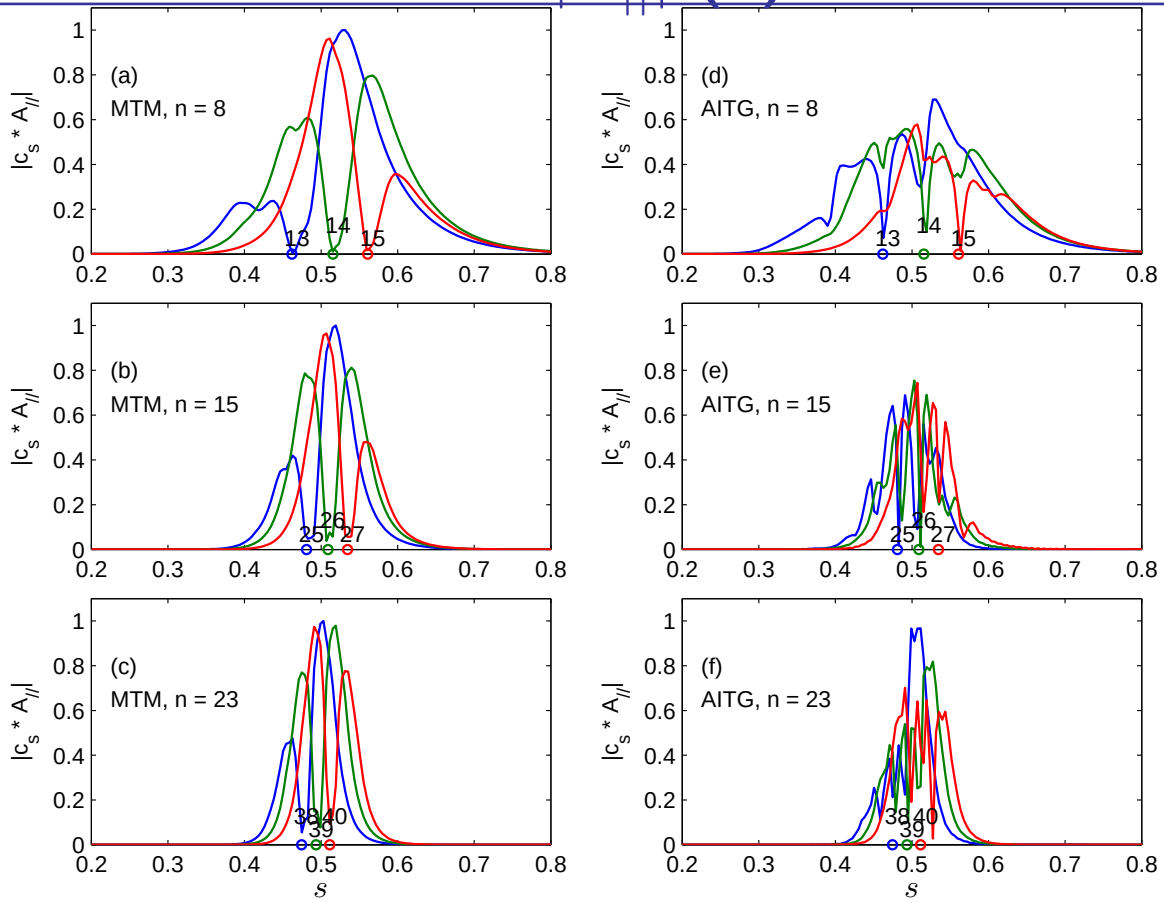

- $|A_{||,m}(r)|$: Three polodial modes with largest relative amplitudes is shown for both AITG and MTM . Location of mode rational surface (indicated on the x-axis) exactly coincide with the sharp structures.

- Except "symmetry" and "free energy drive", several features are structurally similar between MTM and AITG

Properties : Parity of $Re(\varphi_m), Re(A_{||,m})$ - MTM and AITG (10)

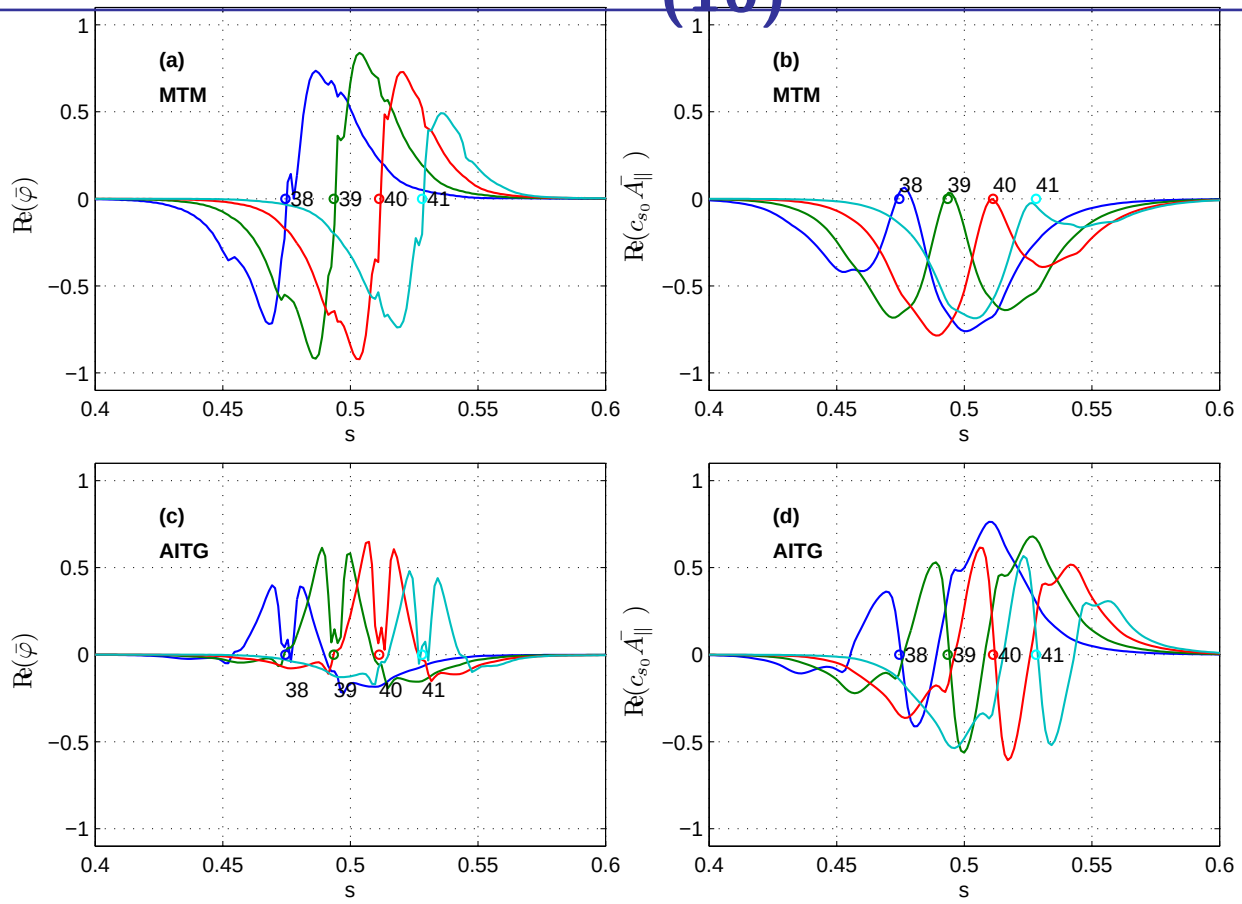

- $Re(\varphi_m(r))$ Vs r for 4 largest amplitude poloidal modes : "Tearing parity" in $\phi_m(r)$ for each m value as well as "envelope" for MTM and "ballooning parity" for AITG

- $Re(A_{||,m}(r))$ Vs r : Parity reversal. Presence of MRS where "cylindrical" $k_{||m,n} = \frac{(m-nq(s))}{Rq} \simeq 0$ brings sharp radial features

Properties : Effect of Profile Variation on MTM (11)

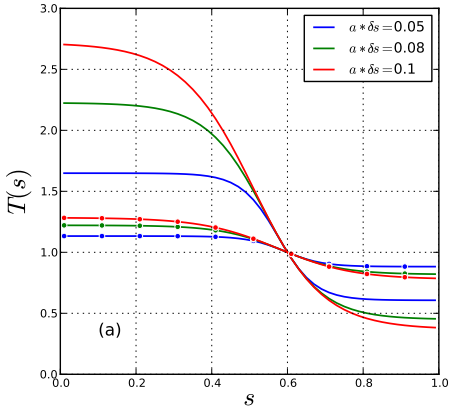

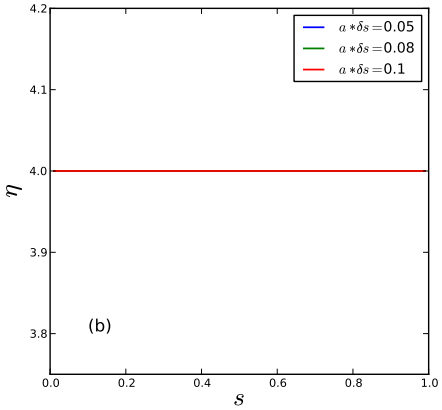

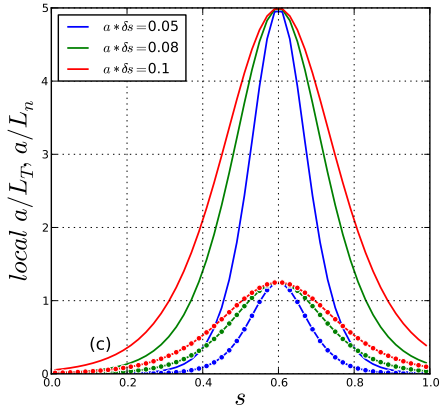

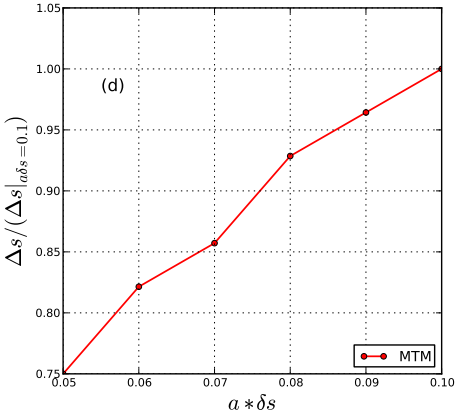

- For system size considered here ($a/\rho_{Li} \simeq 58$), equilibrium profile variation of $n(r)$ and $T(r)$ could be relevant. Fastest growing mode $n = 23$ is considered.

Properties : Effect of Profile Variation on MTM - Mode structures (12)

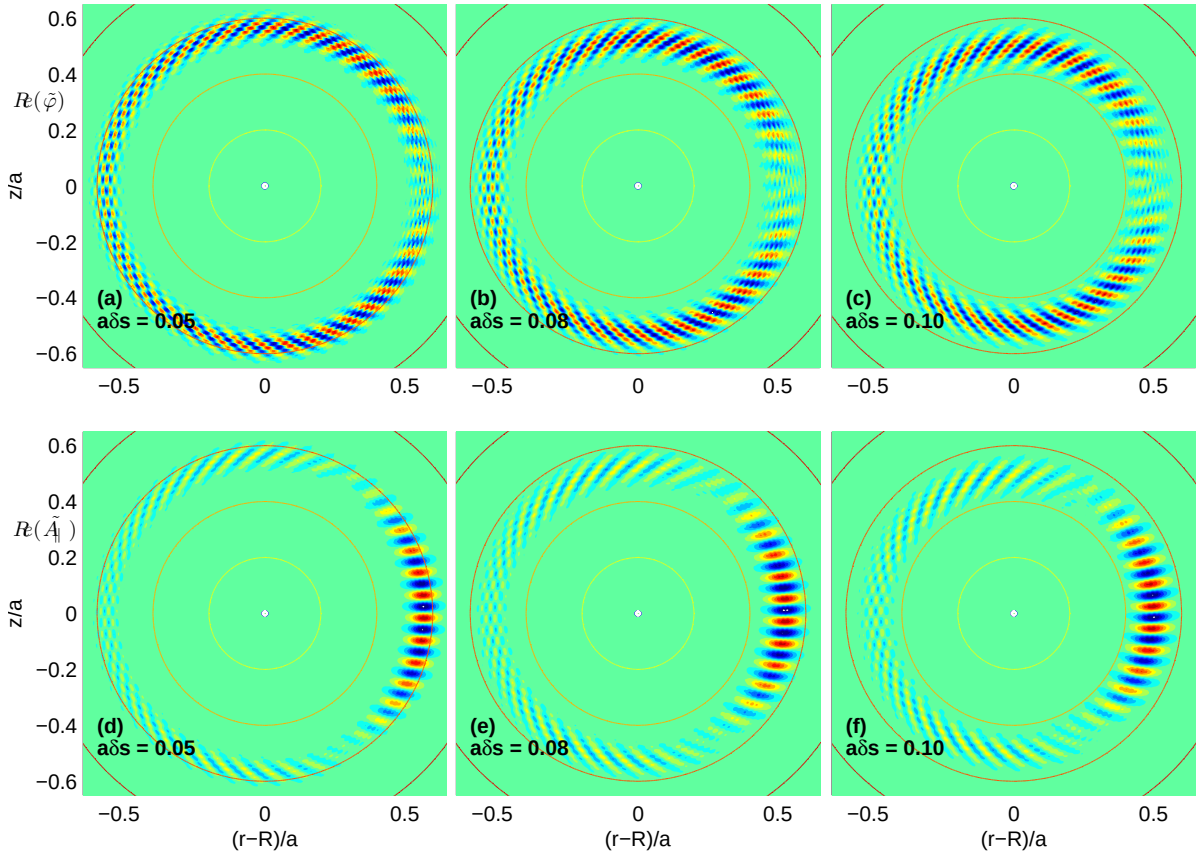

- $a/L_{T,n}$ width decreases from right to left as profiles become "globally" flat. Note that "local" gradients are kept intact at $s = 0.6$ where the mode is localised.
- For the equilibrium studied, Profile effects reduces mode width considerably (by 25%).

Properties : Effect of profile variation on growth of MTM (13)

- Fastest growing MTM $n = 23$ is considered MTM
- Growth rate γ reduces by 20% as profiles become "flat" !

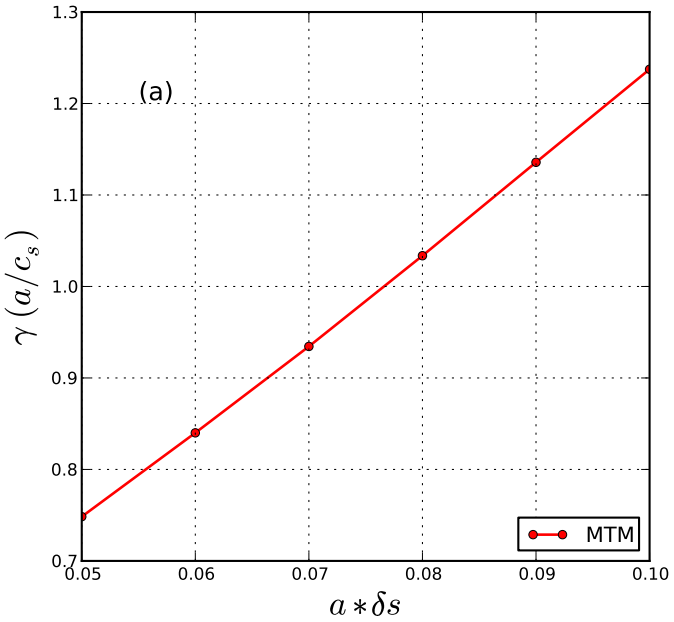

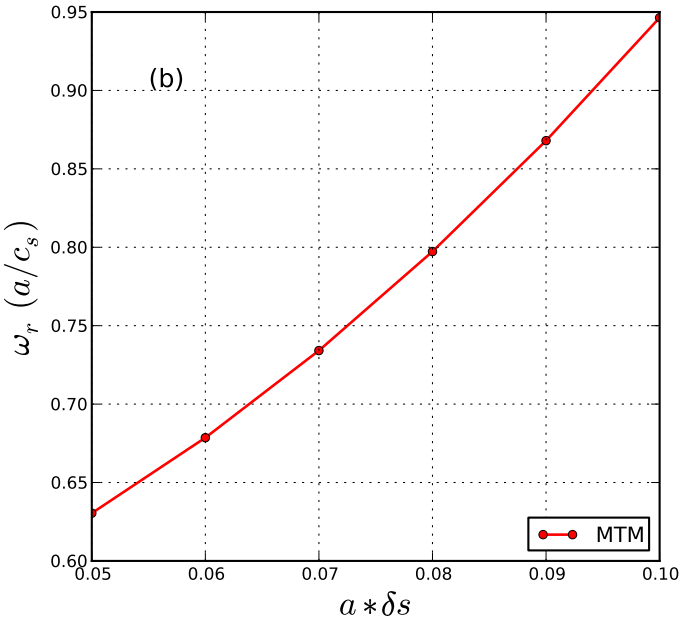

- γ for MTM decreases with "flatter" temperature and density profiles - though $\eta_{i,e}(s)$ is kept constant throughout radial domain.
- For edge pedestal region in large aspect ratio tokamaks, possibility of highly unstable MTMs!. This is consistent with earlier results on edge MTMs, except for collisionality.

Properties : Effect of β variation on growth of MTM (14)

- Mode $n = 23$ is considered for MTM and AITG. For ITG, $n = 8$ is the fastest growing mode for the equilibrium profile considered. $(\eta(s_0)_{i,e} = 4.0)$.

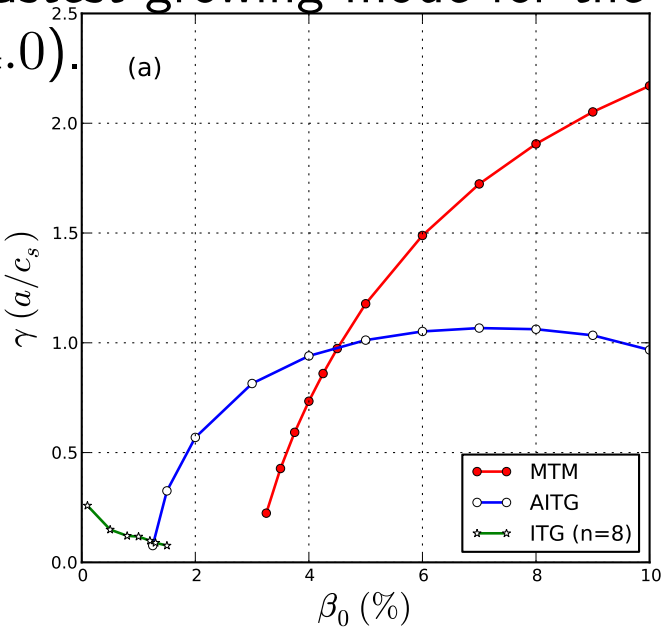

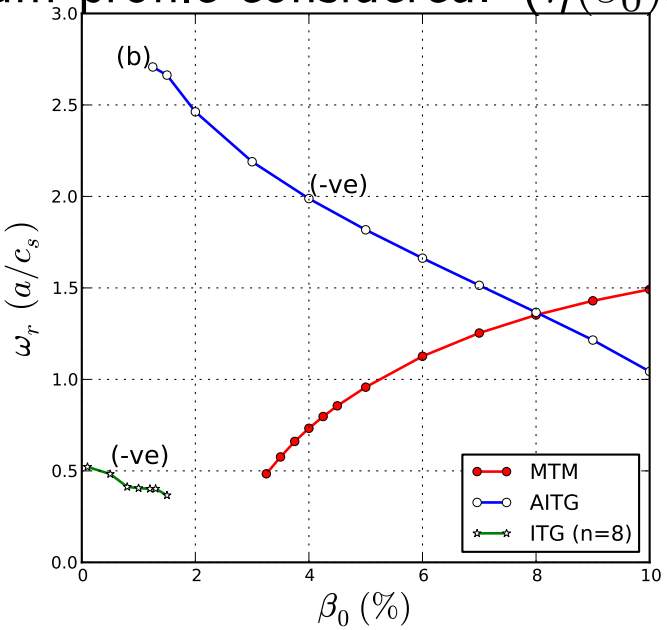

- γ increases with increasing plasma $\beta_0 = \beta(s_0)$
- ITG/AITG rotate in ion diamagnetic direction, while MTM rotates in electron diamagnetic direction. $|\omega_r|$ $increases$ with β_0 for MTM and $decreases$ for AITG
- While ITG stabilizes with increasing β, both MTM and AITG grow. β_{crit} is lower for AITG whereas at larger β values, γ is larger for MTM.

Properties : Mode structure average mode numbers, fluctuation strengths (15)

- Mode $n = 23$ is considered for MTM and AITG. $\eta(s_0)_{i,e} = 4.0$.

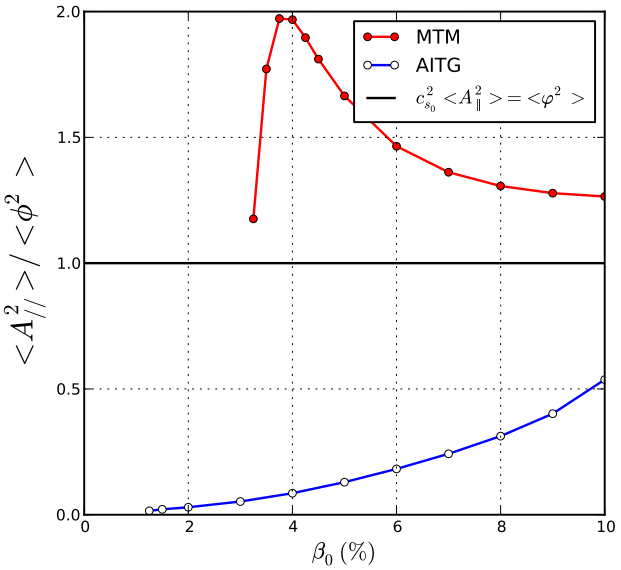

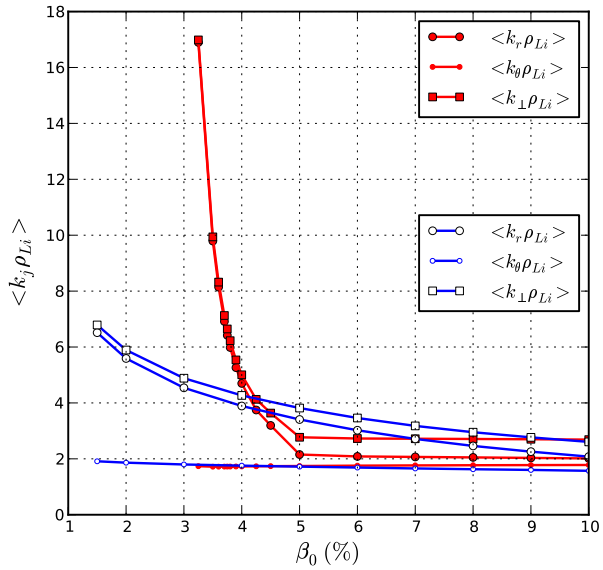

- (Left) For AITG $< A_{||}^2 > / < \varphi^2 > \leq 1$ throughout, MTM is strongly electromagnetic.

- (Right) $< k_r \rho_L i >, < k_\theta \rho_{Li} >, < k_\perp \rho_{Li} >$ is greater than 2. As $\beta \rightarrow \beta_{crit}$, for MTM, perp mode numbers increase beyond 16 nearly reaching electron scales.

- This model considers only $A_{||}$ and φ. For more accurate high β effects, role of $B_{||}$ also has been considered but with very little effect (not shown here).

Properties : Stability Diagram for MTM (16)

- Mode $n = 23$ is considered for MTM.

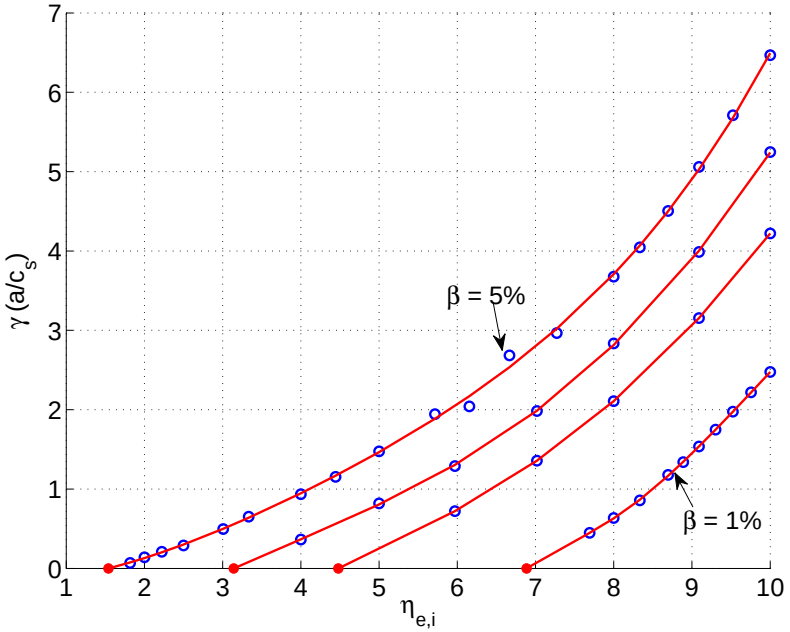

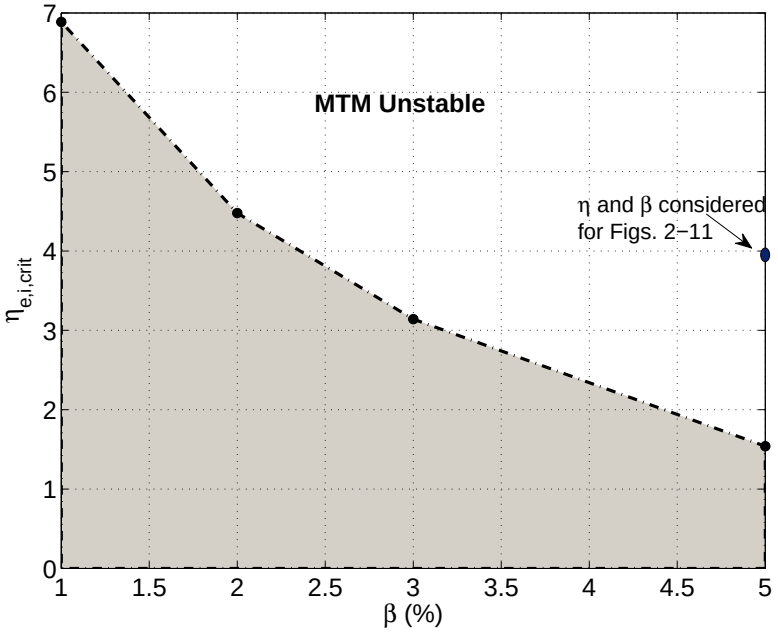

- (Left) γ Vs $\eta_{e,i}$ shows an inverse relationship between $\eta_{i,e}^{crit}$ and β. Red Circles are extrapolated.
- (Right) Stability diagram for MTM : β - $\eta_{i,e}$ space clearly demonstrating the inverse relationship!
- For ITER-like devices, which are expected to go beyond $\eta_{i,e} \geq 4$ at $\beta \simeq 2\%$, one can expect MTM to become unstable and open up nonlinearly electron channel of transport.

Properties : Role of electron temperature gradient - MTM (17)

- Mode $n = 23$ is considered for MTM.

(a)

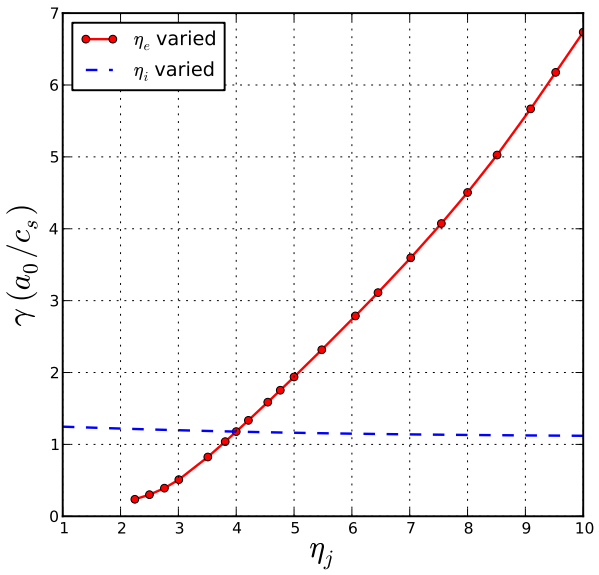

(b)

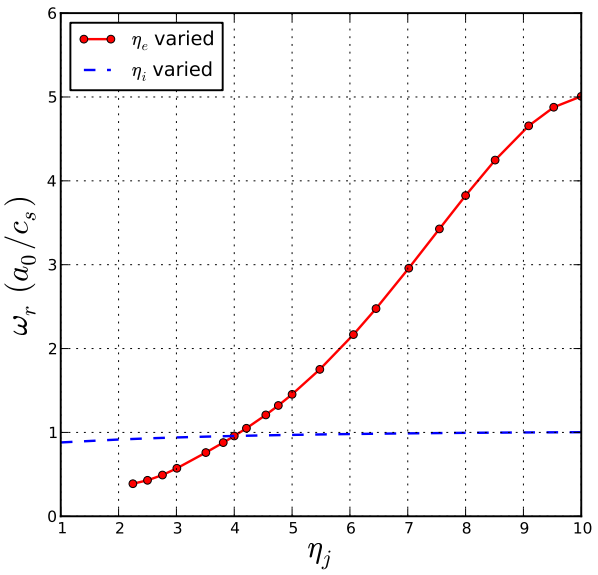

- (Left) γ Vs $\eta_{e,i}$: Blue curve indicates γ variation with η_i for $\eta_e = 4$. Red curve indicates η_e variation for $\eta_i = 4$.
- (Right) ω_r Vs $\eta_{e,i}$: Blue curve indicates γ variation with η_i for $\eta_e = 4$. Red curve indicates η_e variation for $\eta_i = 4$.
- This numerical expt clearly demonstrates that MTM is triggered by electron temperature gradient above a critical β.

Properties : Role of Magnetic Drift of Passing electrons in destabilizing MTM(18)

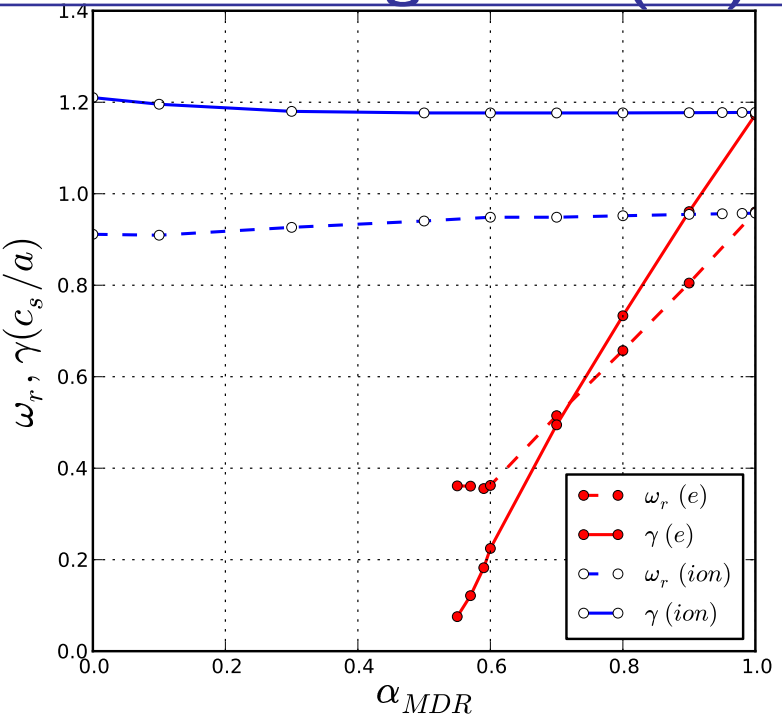

- The Magnetic Drift Resonance term in the Propagator $\mathcal{P}$ for ions and electrons is multiplied by an artificial parameter α_{MDR} which is scaled from 1.0 to 0.0 Aditya K Swamy et al, Phys. Plasmas 21, 082513 (2014)
- MTM is found to be insensitive to ion Magnetic Drift (Blue line/dashed line).
- MTM is completely stabilized by suppressing passing electron Magnetic Drift. (red line/dashed line).

PROPERTIES OF MTM : ROLE OF TRAPPED ELECTRONS

Properties : Variation of γ, ω_r with Toroidal mode number n (1)

- For the same equilibrium profiles, growth rate γ (left) and real frequency ω_r (right)- for MicroTearing Mode (Red) and MTM-TE (Blue)

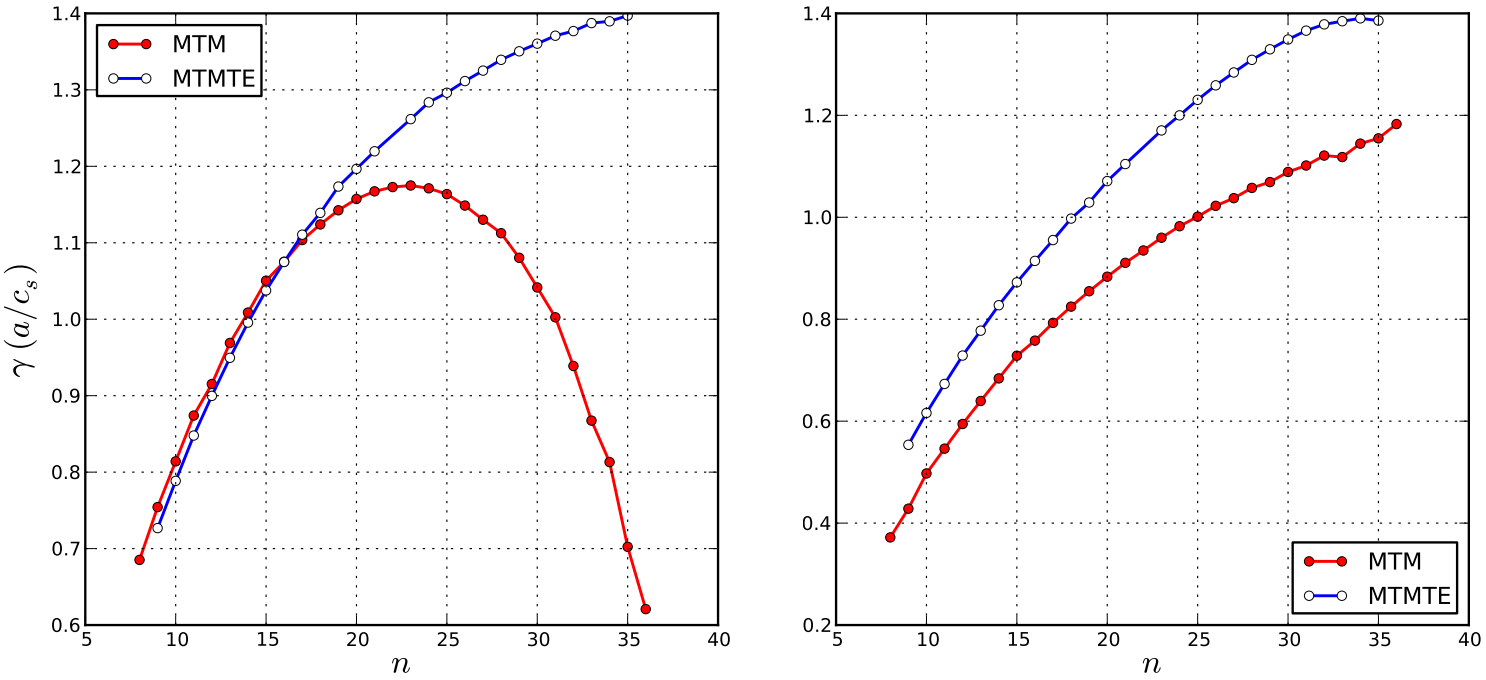

- Inclusion of Trapped Electrons (TE) increases the growth at short scales ($A = 4.0$). [Aditya K Swamy et al, PoP (2015)]
- Poisson Equation is used so that Debye Shielding is included.
- Trapped electron nonadiabatic effect further tends to destabilize high n modes.

Properties : Aspect Ratio Study (1)

- For weakly collisional MTMs studied in the context of spherical Tokamaks, it is reported that [eg. Dickensen et al 2013] only trapped electrons in the presence of weak collisions, drive MTM unstable.

- For completely collisionless MTMs in large aspect ratio Tokamaks, it was found [Aditya K Swamy et al (2014)], that magnetic drift resonance of passing particles alone is sufficient to drive MTM unstable.

- To address this issue, atleast partially, the effect of trapped electrons on collisionless MTMs for various aspect ratios, which strongly control the trapped particle fraction should help.

- Minor radius "a" and equilibrium profiles were kept "constant" and major radius R was varied.

  [Strictly speaking this is a bit unorthodox! Normally to keep k_θ constant throughout aspect ratio variation, quantities Rq and n/R are "held constant" along with "a" while changing R. More on this later.]

Properties : Aspect Ratio Study of MTM-TE (2)

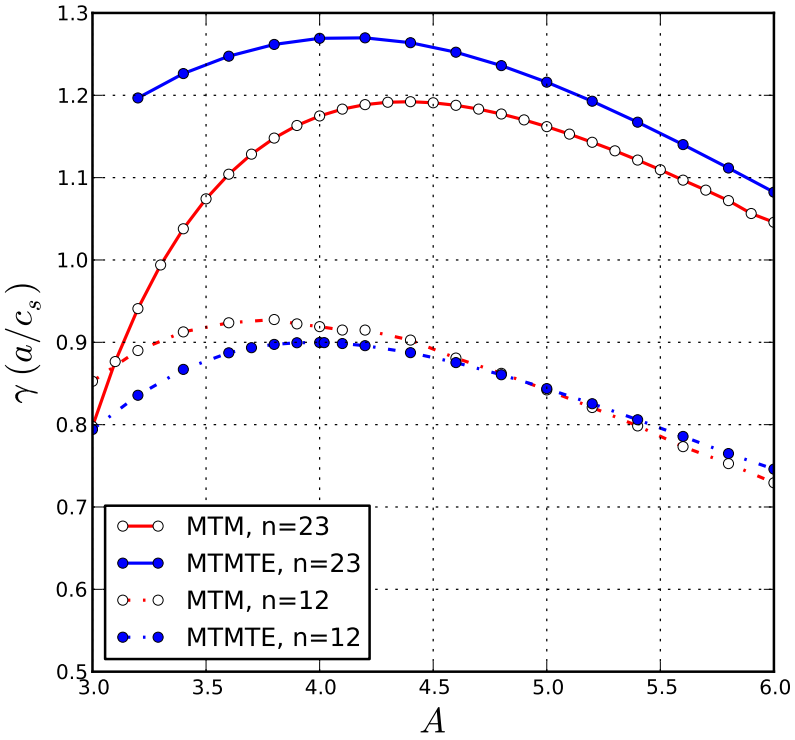

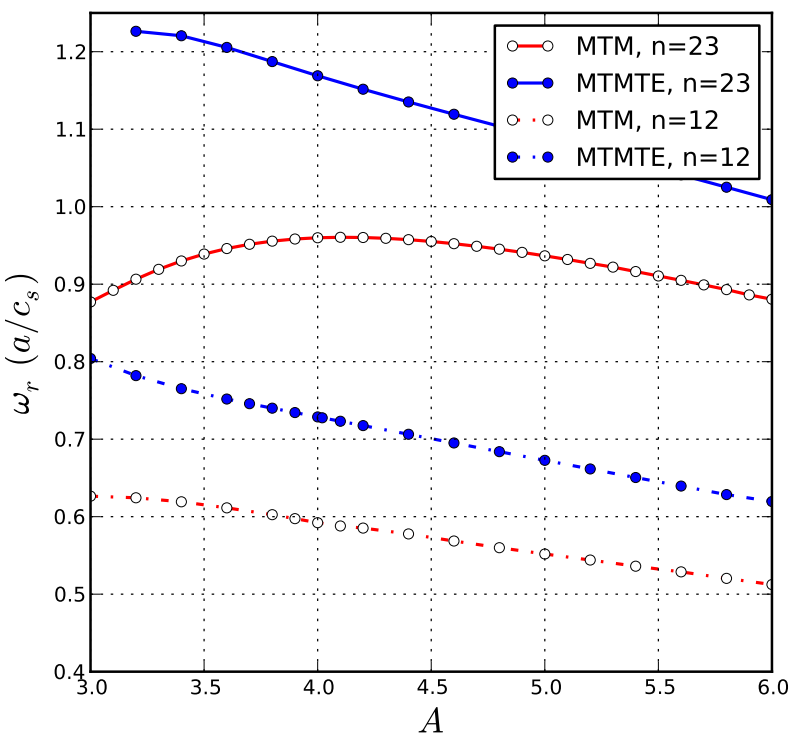

- Trapped Electrons physics becomes predominant at lower aspect ratios. [Dickensen et al PPCF (2013)].
- At large aspect ratios, the magnetic drift resonance of passing electrons appear to be the dominant effect.
- Results are qualitatively consistent with past work in tight aspect ratio devices.

Properties : Aspect Ratio Study of MTM-TE (3)

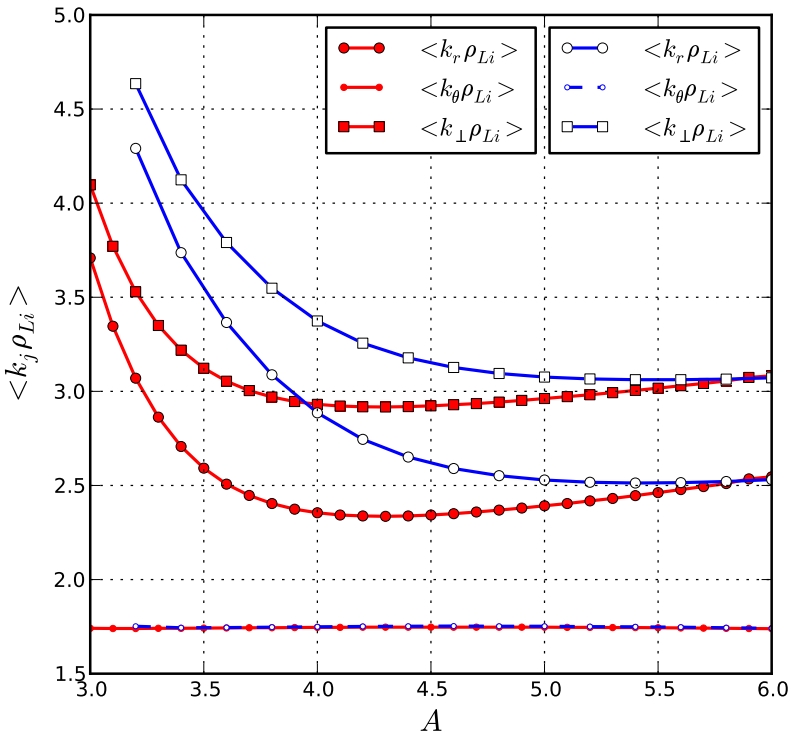

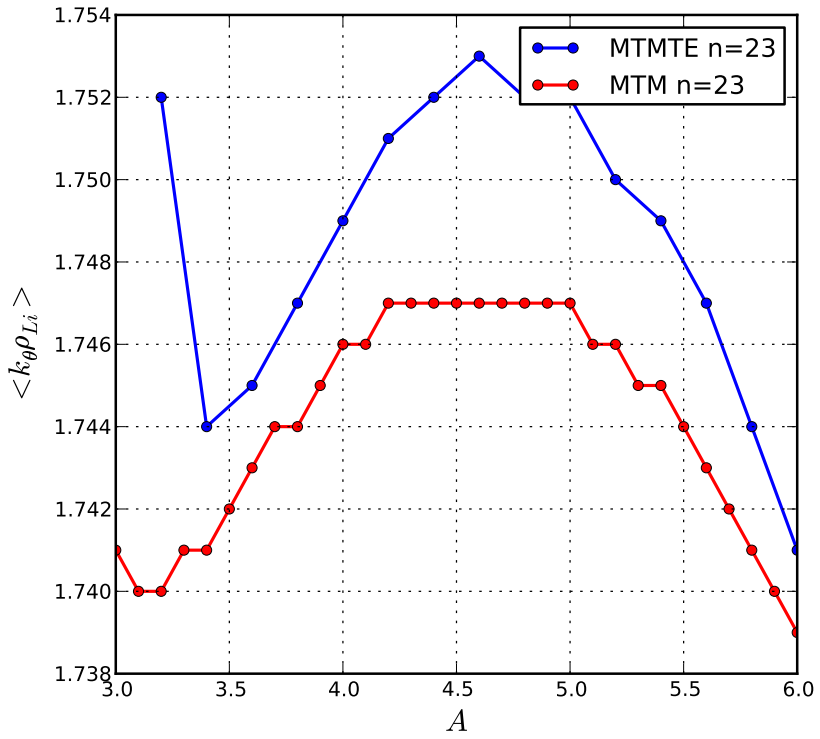

- Throughout, $< k_\theta \rho_{Li} >$ has very little varation as function of aspect ratio A.
- Zoomed picture of $< k_\theta \rho_{Li} >$ Vs A on the right showing about a maximum of 0.7% variation when aspect ratio A is varied.

Properties : Mode structure φ as function of Aspect Ratio (3)

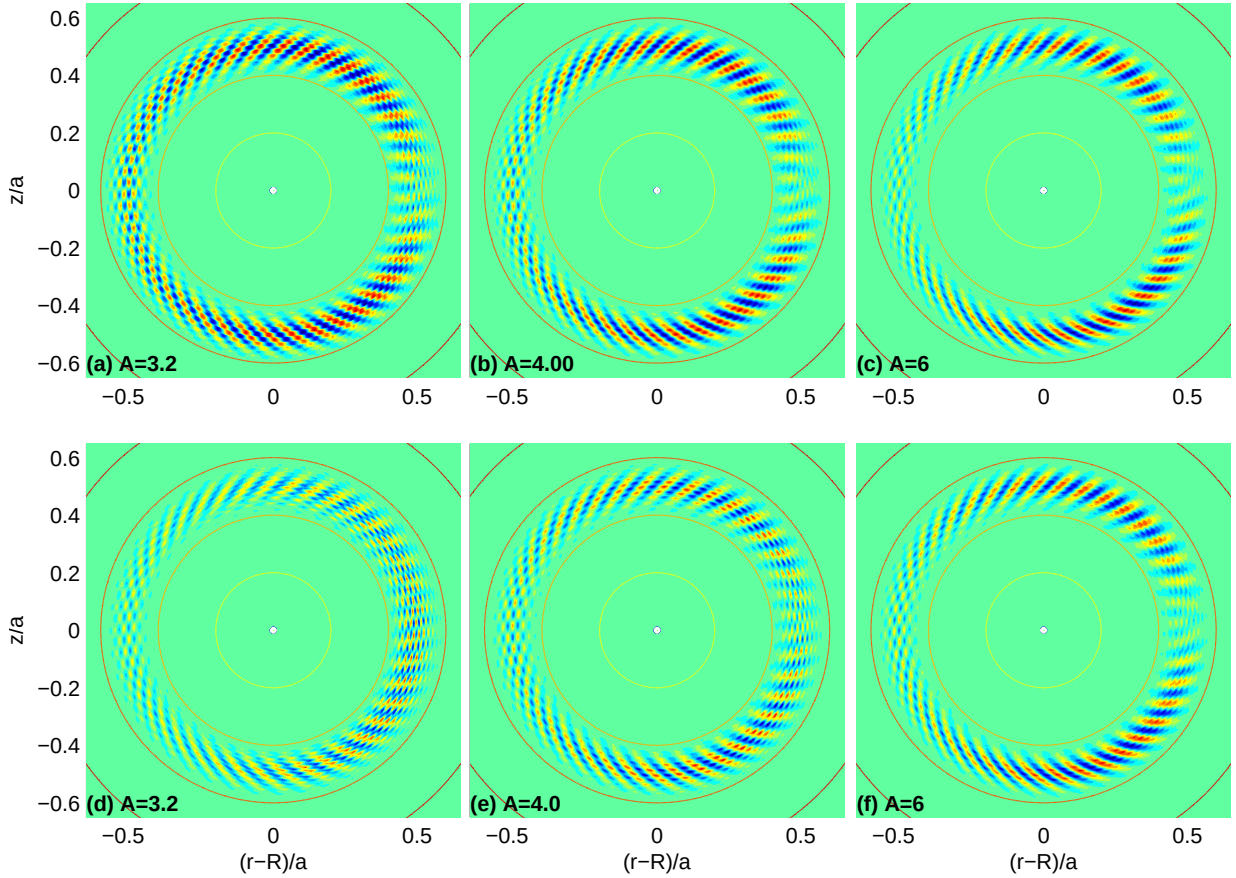

- For $n = 23$: Aspect Ratio $A = R/a$ $(a = 0.5\ m)$. Pure MTM $\varphi(r, \theta)$ (top row).
- MTM-TE Eigenmode $\varphi(r, \theta)$ (bottom row) is shown for 3 values of R (or A)
- Parity of φ is retained throughout the Aspect Ratio Scan.

Properties : Mode structures as function of Aspect Ratio (4)

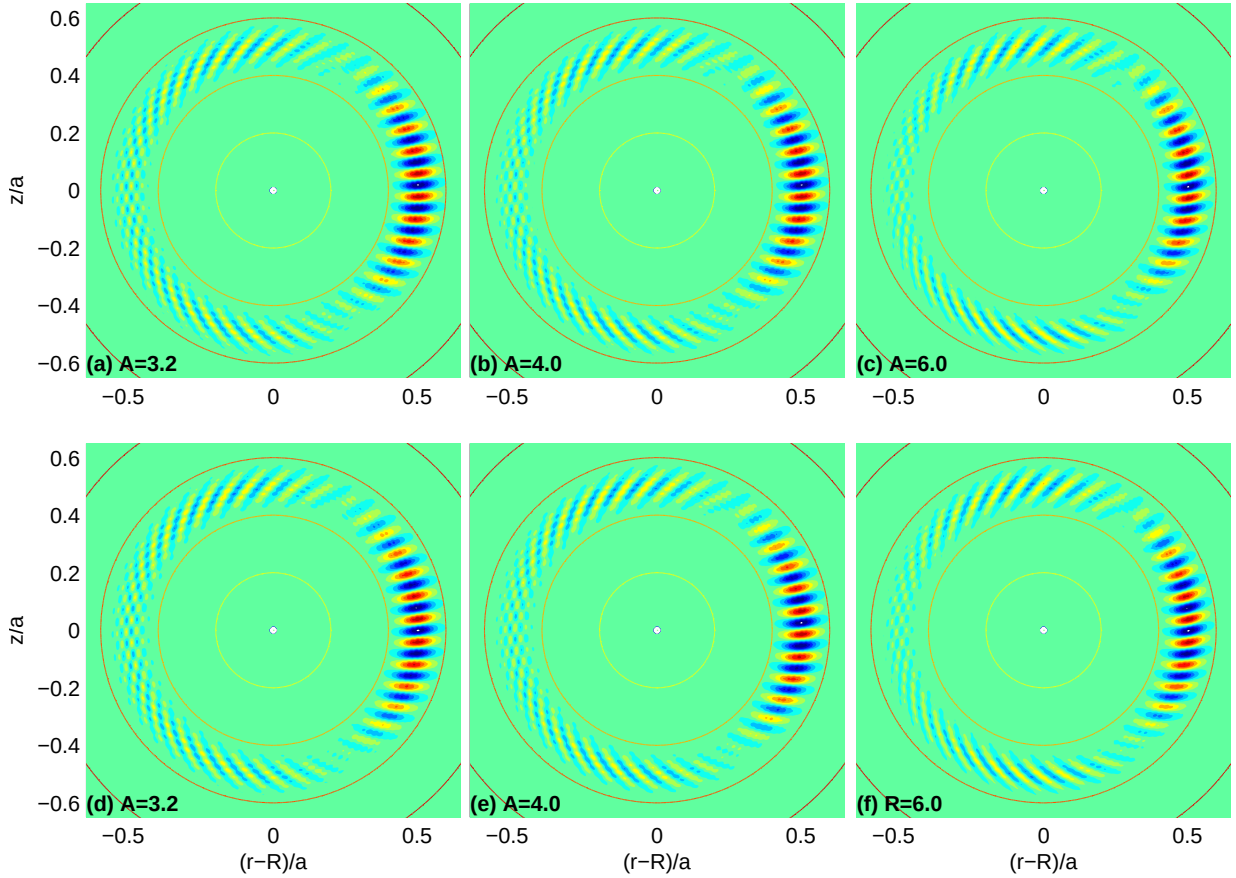

- For $n = 23$: Aspect Ratio $A = R/a \;\; (a = 0.5\, m)$. Pure MTM $A_{||}(r, \theta)$ (top row).
- MTM-TE Eigenmode $A_{||}(r, \theta)$ (bottom row) is shown for 3 values of R (or A)
- Parity of $A_{||}$ structure is retained throughout the Aspect Ratio Scan.

Properties : Variation of γ, ω_r with β (1)

- Growth rate γ (left) and real frequency ω_r (right)- for MicroTearing Mode (Red) and MTM-TE (Blue) for toroidal mode numbers $n = 10, 12, 23$

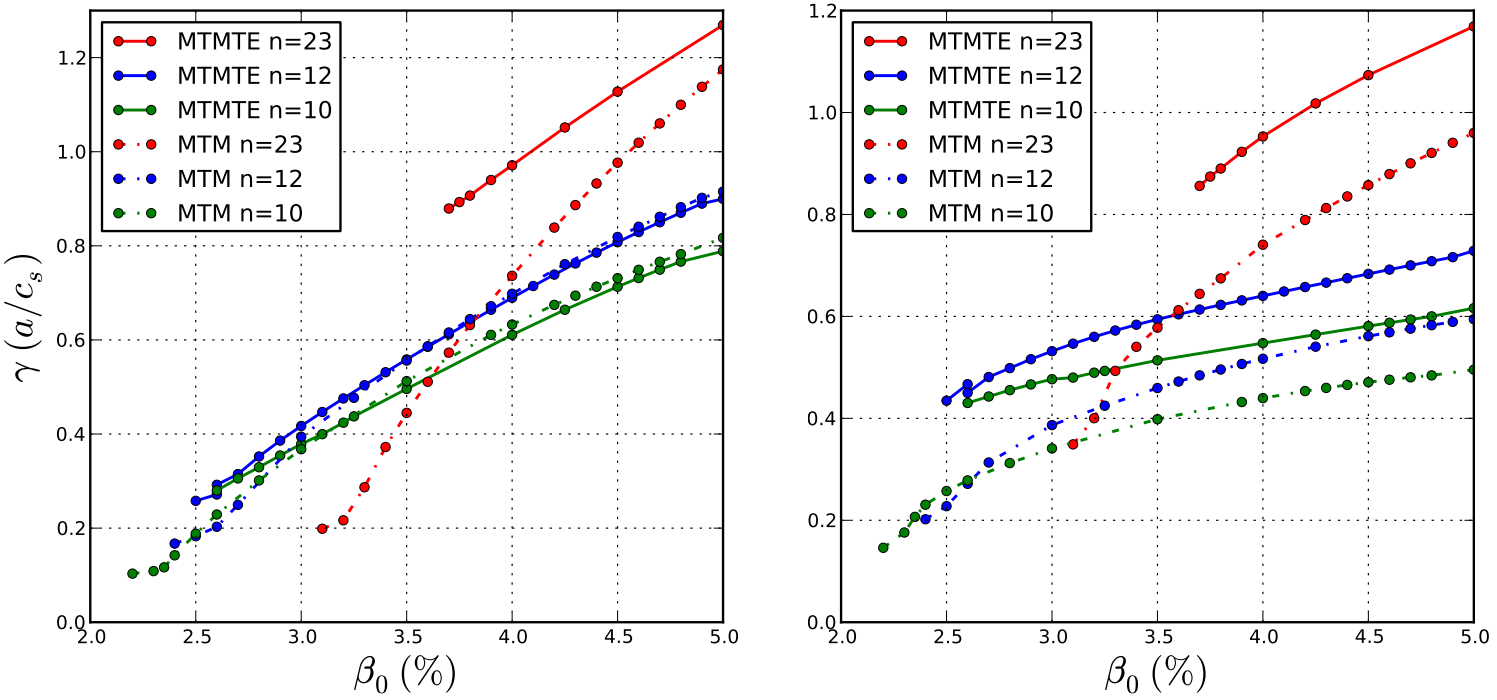

- Trapped Electrons (TE) increases the growth at short scales ($A = 4.0$).
- Poisson Equation is used so that Debye Shielding is included.
- Low n modes have lower β_{crit}. [Aditya K Swamy et al, PoP (2015)]

Properties : Variation of γ, ω_r with β (2)

- As critical β is approached, $< k_r \rho_{Li} >$ (and hence $< k_\perp \rho_{Li} >$)spectrum increases enormously.

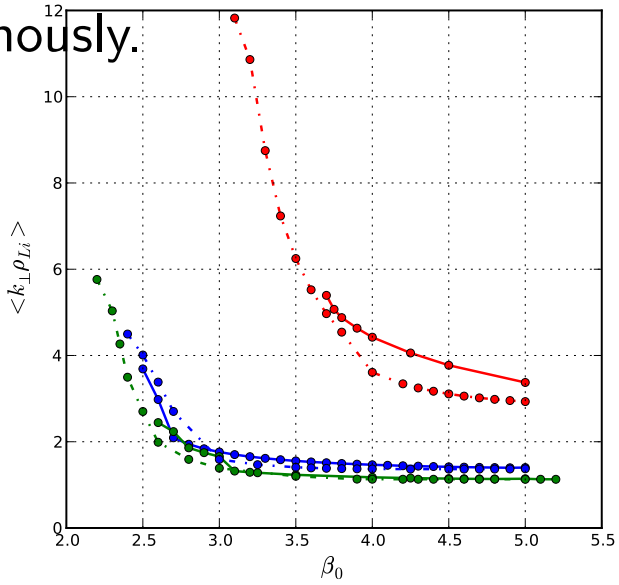

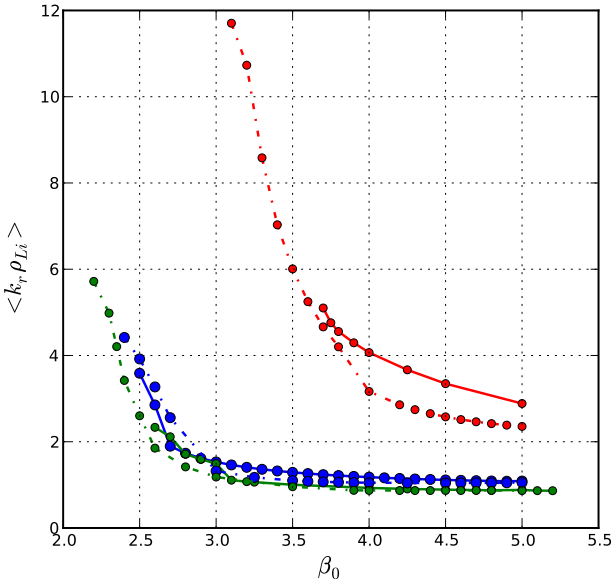

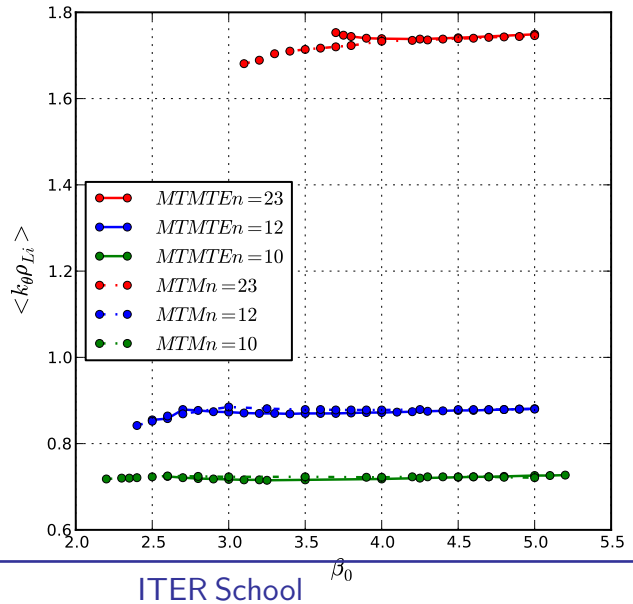

PROPERTIES OF MTM : ROLE OF $q-$PROFILE

MTM - q profile studies

- How does q-profile and the resulting magnetic shear affect MTMs and other modes?

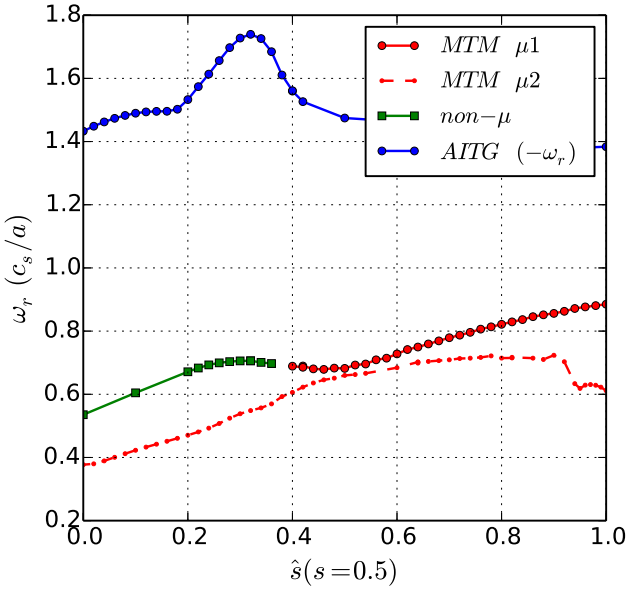

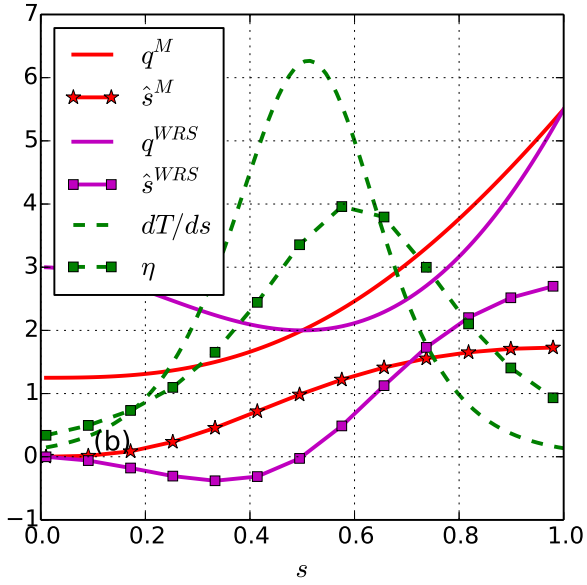

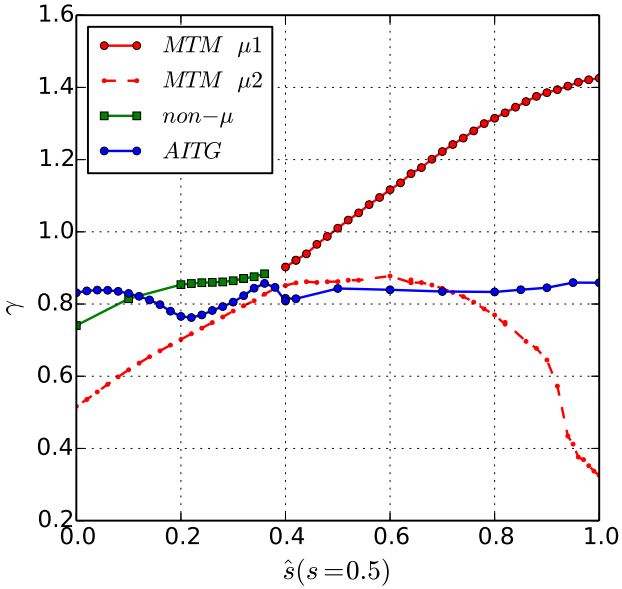

- Start from "conventional" $q-$profile and "continously" change profiles to keep track of "all" the unstable modes (ω_r, γ)!

MTM : Effect of weak magnetic shear $\hat{s}$

- Mode structures of MTMs ($\mu-$ modes) and mixed parity modes (non-μ modes)

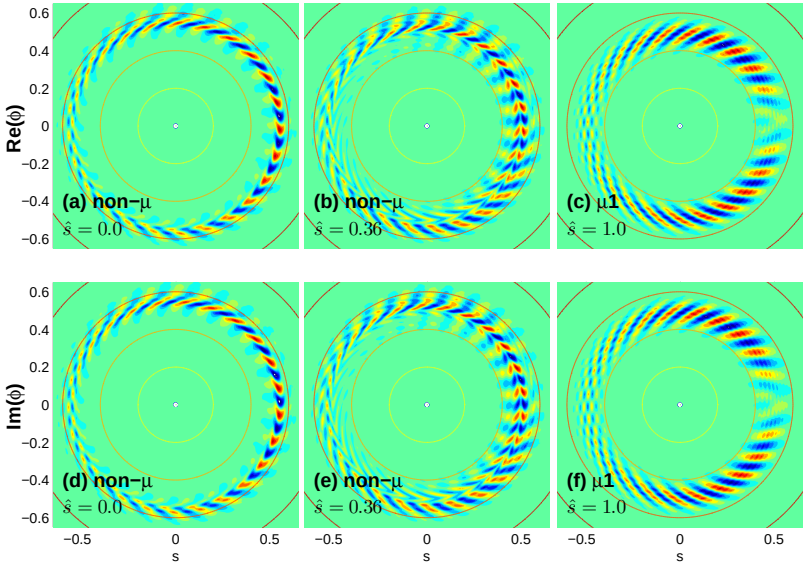

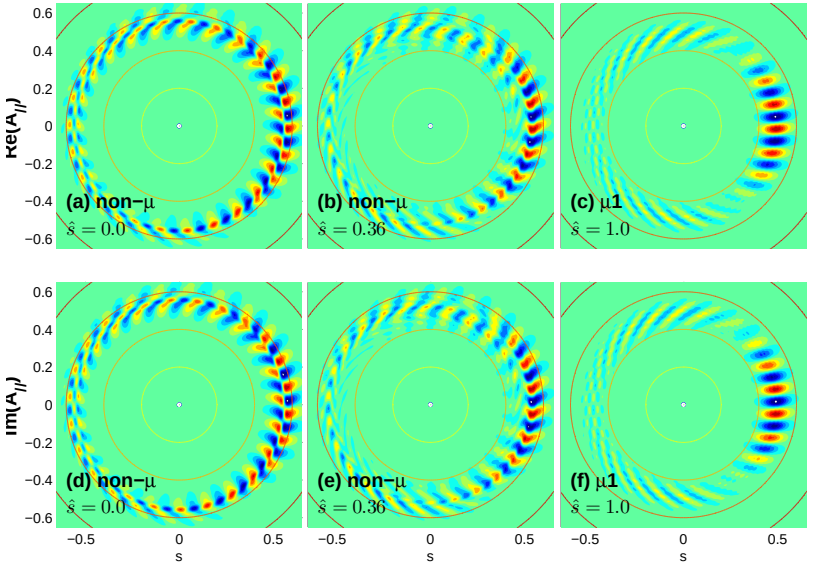

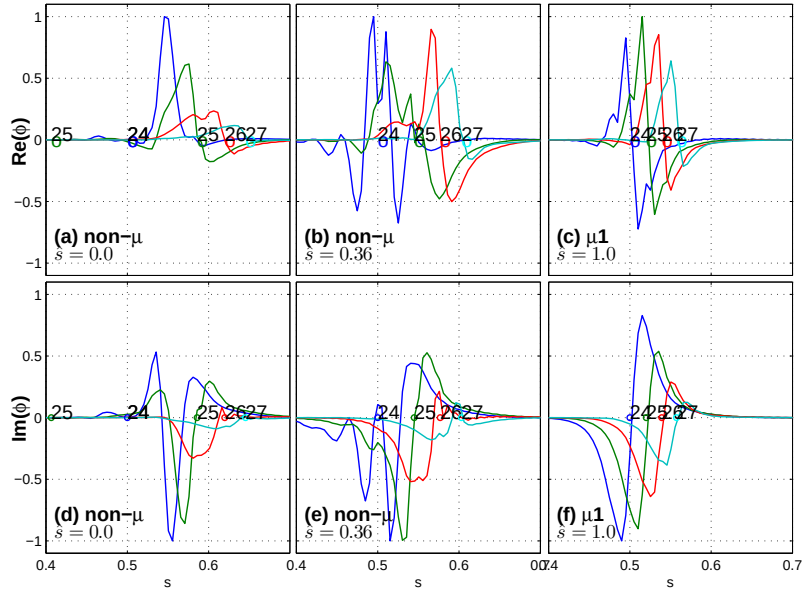

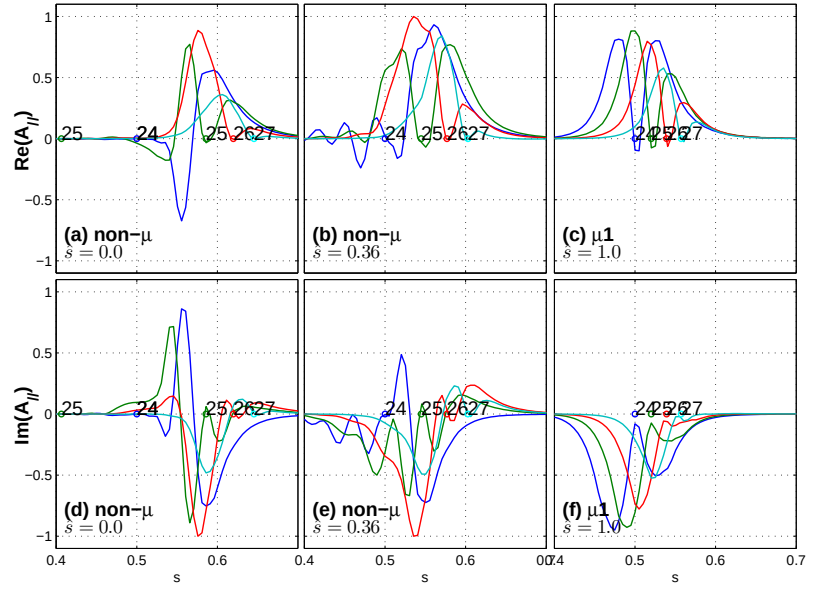

MTM : Effect of weak magnetic shear $\hat{s}$ (2)

- Multipe modes: $n-$ scan (top row) and $\beta-$scan (bottom row).

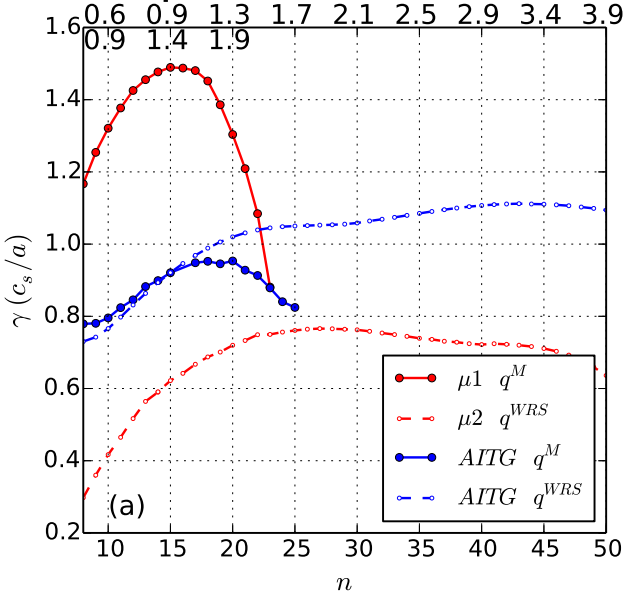

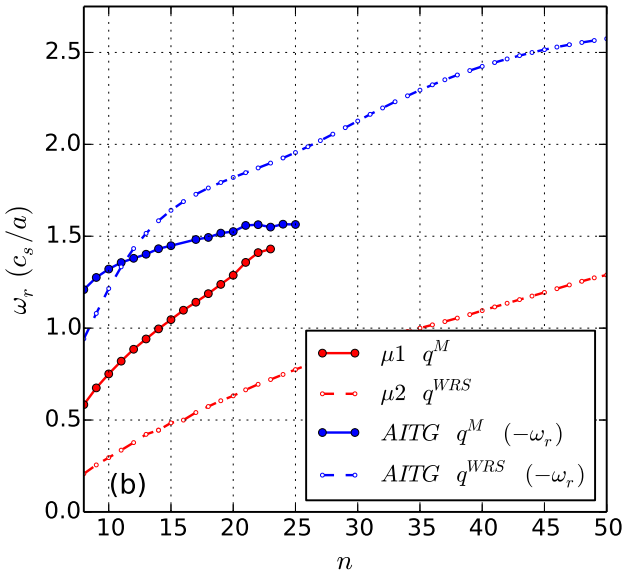

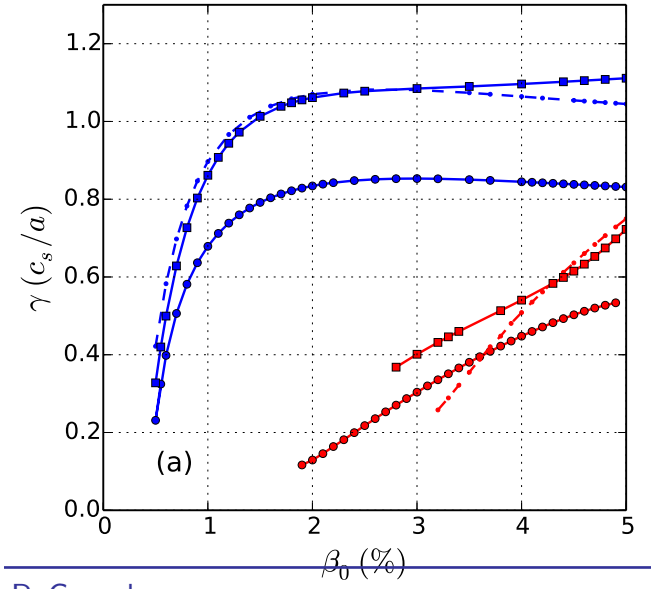

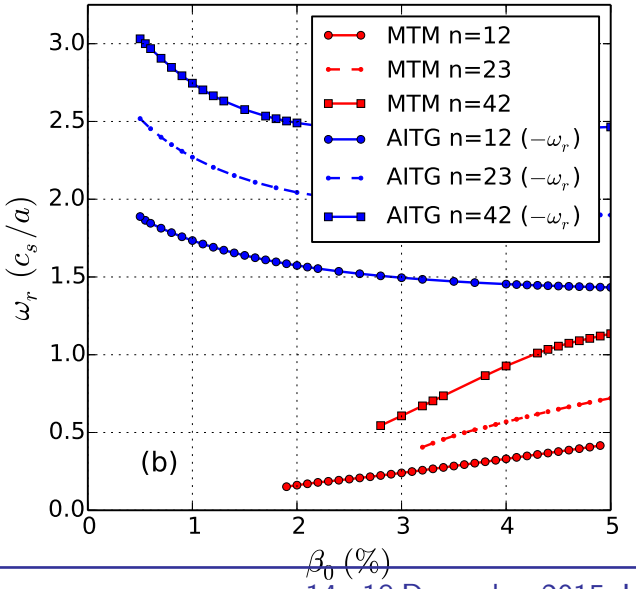

MTM : Effect of weak magnetic shear $\hat{s}$ (3)

- MTMs are sensitive to positive magnetic shear $\hat{s} > 0$ and the location of $\frac{dT_{eq}(r)}{dr}$

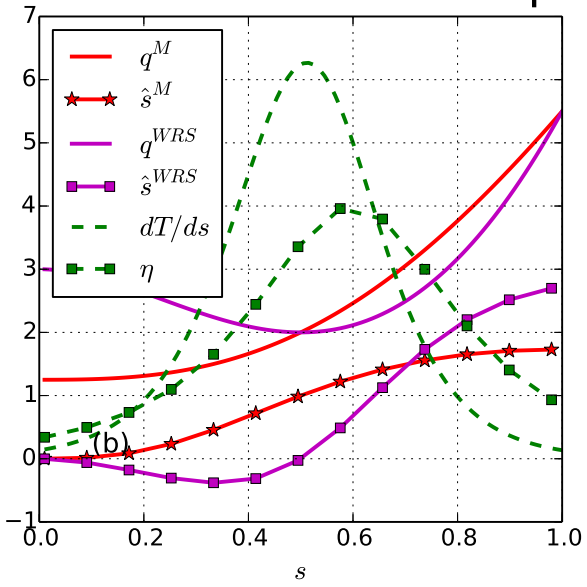

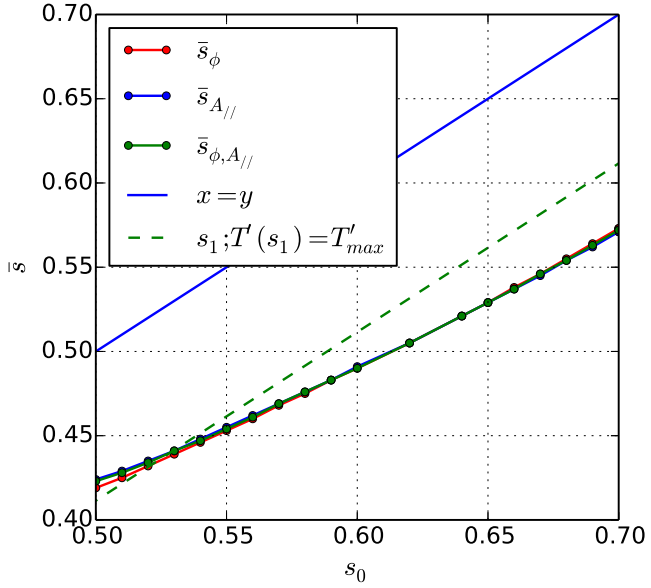

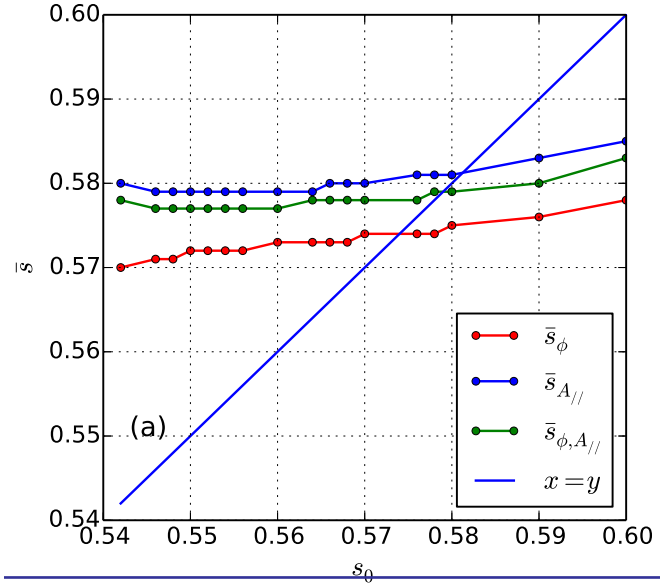

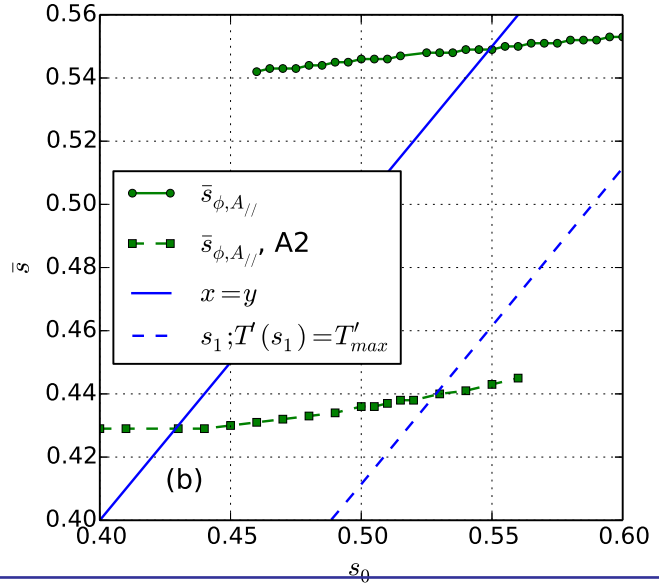

MTM : Outlook & Issues (1)

- Considering only the passing electrons, completely collisionless unstable MTMs are found in Large Aspect Ratio hot tokamaks for a broad range of relevant parameters namely $\beta \simeq 1\% - 5\%$ and $a/L_{Te} \simeq 1.5 - 12.5$
- Instability drive is found be due to electron magnetic drift resonance in the presence of electron temperature gradient and β above β_{crit}
- Global 2D mode structures were obtained for both MTM and AITG (or KBM) for the same set of equilibrium profiles and parameters.
- $A_{||}$ fluctuations for MTM show "even parity" or "tearing parity" around a MRS and the "envelope" of several such modes also exihibits an "even parity" w.r.t radial location of the peak amplitude. φ fluctuations show "odd parity.

MTM : Outlook & Issues (2)

- Radially averaged modes of MTM and AITG show a parity swap along θ with respect to $\theta = 0$.

- For the equilibrium considered, the fastest growing modes are short wavelength modes.
  $< k_\theta \rho_{Li} > \simeq 0.75 - 2.5, \quad < k_r \rho_{Li} > \simeq 0.9 - 3.5, \quad < k_\perp \rho_{Li} > \simeq 1.0 - 4.0$

- At $\eta_{i,e} = 4$, for large aspect ratio collisionless hot Tokamaks, β_{crit} above which MTM is unstable is $2 - 2.5\%$.

- A stability diagram showing an inverse relationship between β and η_{crit} is demonstrated. For example, hot large aspect ratio Tokamaks with small β would require larger $\eta_{i,e}$ to destabilize collisionless MTMs and vice versa.

MTM-TE : Outlook & Issues (3)

- For large aspect ratio collisionless MTM, addition of Trapped Electrons alters the growth and real frequency.
- High k limit gets qualitatively modified with Trapped Electrons.
- Aspect Ratio Scan clearly demonstrates that
  - At Large Aspect Ratio, the magnetic drift resonance of passing electrons is important.
  - As Aspect Ratio is reduced, the physics of trapped electrons tend to dominate over passing electrons - consistent with results found in Spherical Tokamaks.
  - Formulation is Large Aspect Ratio. Hence the results at small aspect ratio should be regarded as suggestive.

MTM-TE : Outlook & Issues (4)

- Study by variation of β at a given aspect ratio, clearly demonstrates that
  - For lower n values, β_c is lower!
  - As β approaches smaller values, it is found that k_r spectral demands increase.
  - When trapped electrons are included, below a certain β value, a spurt of multiple modes are found by continously tracking the trapped electron fraction.
  - A jump in ω_r and a continous but nonmonotonic change in γ, could possible indicate mode-conversion to finite β TEM or simply a multi-mode coexisitence?
- The correctness of MTM-TE results is demonstrated by showing that the mode structure is retained throughout the aspect ratio scan.

MTM-TE : Outlook & Issues (5)

- $B_{||}$ effects are all, but minimal (not shown here).
- For a variety of temperature profiles and q-profiles, resulting in a range of drive values - relatively weak to large and for a range of shear values, MTM and MTM-TE has been demonstrated to survive. Mixed parity modes exist and depend strongly on magnetic shear.
- An important equilibrium finite-β effect is Shafranov Shift. This has not been addressed here.
- Effect of poloidal shear flows and toroidal flows on MTM and MTM-TE is also not included.
- Are collisional MTMs (core and edge) and collisionless MTMs (addressed here) - same branches Or different branches of a tearing parity mode? Inclusion of a Landau-Boltzmann-like collision operator should help.

THANK YOU

BACKUP SLIDES

Global linear gyrokinetic theory (1)

- Vlasov Eqn for species j :

$$\frac{D}{Dt}f_j(\vec{r},\vec{v},t) \equiv \frac{\partial f_j}{\partial t} + \vec{v}\cdot\vec{\nabla}f_j + \frac{q_j}{m_j}(\vec{E}_T + \vec{v}\times\vec{B}_T)\cdot\vec{\nabla}_v f_j = 0$$

- $\vec{E}_T$ and $\vec{B}_T$ are total electric and magnetic fields to be obtained from Max. Eqns
- Assume an "equilibrium" without a zeroth order E-field and with zeroth order magnetic field $\vec{B}$.
- For small perturbation $\tilde{E}$ around this "equilibrium" one can expand $f_j = f_{0,j} + \tilde{f}_j$ such that $\tilde{f}_j/f_{0,j} \ll 1$
- Thus zeroth order eqn is :

$$\left.\frac{D}{Dt}\right|_{u.t.p.} f_{0j}(\vec{r},\vec{v},t) = 0 \quad where \quad \left.\frac{D}{Dt}\right|_{u.t.p.} \equiv \frac{\partial}{\partial t} + \vec{v}\cdot\vec{\nabla} + \frac{q_j}{m_j}(\vec{v}\times\vec{B})\cdot\vec{\nabla}_v$$

Global linear gyrokinetic theory (2)

- First order eqn is

$$\left.\frac{D}{Dt}\right|_{u.t.p.} \tilde{f}_j(\vec{r},\vec{v},t) = -\frac{q_j}{m_j}\tilde{E}\cdot\vec{\nabla}_{\vec{v}} f_{0j}$$

- Here "u.t.p." implies "unperturbed trajectory of particle" meaning equilibrium trajectories of particles

- Within a "linear" theory, the effect of perturbation does not "back react" and change the equilibrium features.

- Express $\tilde{E}$ in terms of $\tilde{\varphi}$, $\vec{B}$ in terms of $\vec{A}$, define change of variables $(\vec{r},\vec{v}) \rightarrow (\vec{r},\xi = v^2/2, \mu = v_\perp^2/2B, \psi_0)$. This helps express velocity degrees of freedom in terms of single particle constants of motion.

- Using particle canonical angular momentum for species j, i.e., $\psi_{0j} = \hat{e}_\phi \cdot \left[\vec{r}\times(\vec{A} + m_j\vec{v}/q_j)\right] = \psi + m_j r v_\phi/q_j$, one can write $f_{0j}(\vec{r},\vec{v}) = f_{0j}(\vec{r},\xi,\mu,\psi_{0j})$. Here cylindrical co-ordinates $\vec{r} \equiv (r,\phi,z)$ have been introduced and $\psi = rA_\phi$ is the poloidal flux function per unit radian. Such a transformation would enable one to express f_{0j} in terms of single particle constants of motion.

Global linear gyrokinetic theory (3)

- In the new variables, $\nabla_v f_{0j}$ term on the right hand side $(r.h.s)$ of first order equation becomes

$$\nabla_v f_{0j}(r,\xi,\mu,\psi_{0j}) = v\left(1+\frac{m_j r v_\phi}{q_j}\frac{\partial}{\partial\psi_{0j}}\right)\frac{\partial f_{0j\psi}}{\partial\xi}+\frac{v_\perp}{B}\frac{\partial f_{0j\psi}}{\partial\mu}+\frac{m_j r\hat{e}_\phi}{q_j}\frac{\partial f_{0j}}{\partial\psi_{0j}}\bigg|_{\psi_0=\psi}$$

  where $f_{0j\psi}\equiv f_{0j}(\psi_{0j}=\psi)$ and $\hat{e}_\phi$ is the toroidal unit vector.

- Similarly using new variables, write perturbed distribution as "adiabatic" response and the "rest"!

$$\tilde{f}_j = h_j^{(0)} + \tilde{\varphi}\frac{q_j}{m_j}\left[\left(1-\frac{v_\phi}{\Omega_{pj}}\nabla_n\right)\frac{\partial f_{0j\psi}}{\partial\xi}+\frac{1}{B}\frac{\partial f_{0j\psi}}{\partial\mu}\right]$$

  Here $h_j^{(0)}$ is the zeroth order term of $h_j = h_j^{(0)}+\frac{1}{w_{cj}}h_j^{(1)}+\frac{1}{w_{cj}^2}h_j^{(2)}$..... Remember that we would like to describe modes with $\omega \ll \omega_{c,j}$ and note that $D/Dt \simeq O(\omega_{cj})$.

Global linear gyrokinetic theory (4)

- Putting the last two equations into first order eqn, we get:

$$\left.\frac{D}{Dt}\right|_{u.t.p} h_j^{(0)}(r,v,t) = -\frac{q_j}{m_j}\left[\frac{\partial f_{0j\psi}}{\partial \xi}\frac{\partial}{\partial t} + \frac{v_{||}}{B}\frac{\partial f_{0j\psi}}{\partial \mu}\hat{e}_{||}\cdot\nabla + \frac{1}{\Omega_{pj}}\nabla_n f_{0j}\Big|_{\psi}\hat{e}_\phi\cdot\nabla\right]\tilde{\varphi} + O($$

  In above equation, we have introduced the following definitions: $\Omega_{pj} = w_{cj}B_p/B$, $w_{cj} = q_jB/m_j$, $B_p = |\nabla\psi|/r$

- Gyroaveraging: In large aspect ratio Tokamak, $v = v_\perp(\hat{e}_\varrho cos\alpha + \hat{e}_\theta sin\alpha) + v_{||}\hat{e}_{||}$, where unit vectors $(\hat{e}_\varrho, \hat{e}_\theta, \hat{e}_\phi)$ define the toroidal coordinates and α is the gyro-angle.

- We define gyro-averaging a quantity "Q" as

$$< Q >= \frac{1}{2\pi}\int_0^{2\pi} d\alpha Q(\alpha; ..)$$

Global linear gyrokinetic theory (5)

- In the perturbed eqn above, the terms in square brackets [..] on the $r.h.s.$ are all $equilibrium\ quantities$ and are independent of α. Thus only the electrostatic potential is to be averaged. Similarly, on the left hand side $(l.h.s)$, h_j^0 is independent of α, hence, only $D/Dt|_{u.t.p}$ is to be gyro-averaged.

- $$\left.\frac{D}{Dt}\right|_{u.t.p} \overset{gyro-averaging}{\Longrightarrow} \left.\frac{D}{Dt}\right|_{u.t.g} \equiv \frac{\partial}{\partial t} + (v_{||}\hat{e}_{||} + v_{dj}) \cdot \frac{\partial}{\partial R}$$

  where $v_{dj} = (v_\perp^2/2 + v_{||}^2)\hat{e}_z/(rw_{cj})$, $u.t.g.$ implies $unperturbed\ trajectory\ of\ guiding\ centers\ R$ defined by $R = r + v \times \hat{e}_{||}/w_{cj}$.

- Similarly the electrostatic potential is to be gyroaveraged, but we dont know the form of ϕ!

$$< \tilde{\varphi} >= \frac{1}{2\pi} \int_0^{2\pi} d\alpha \ [\ \tilde{\varphi}(r[\alpha], t))\ ] \Big|_{r=R-v\times\hat{e}_{||}/w_{cj}}$$

  Since $\tilde{\varphi}(r[\alpha], t)$ is an unknown function, the gyro-averaging is performed by first Fourier decomposing these functions.

Global linear gyrokinetic theory (6)

- Now represent the particle co-ordinate r by gyro-center R and remember that

$$J_p(x) = \frac{1}{2\pi}\int_0^{2\pi} d\alpha \exp[\iota(xsin\alpha - p\alpha)]$$

- The final form of gyrokinetic eqn is

$$\left.\frac{D}{Dt}\right|_{u.t.g} h_j(R,v,t) = -\left(\frac{q_j}{m_j}\right)\left[\frac{\partial f_{0j\psi}}{\partial \xi}\frac{\partial}{\partial t} + \frac{v_{||}}{B}\frac{\partial f_{0j\psi}}{\partial \mu}\hat{e}_{||}\cdot\nabla + \frac{1}{\Omega_{pj}}\nabla_n f_{0j}\Big|_{\psi}\hat{e}_{\phi}\cdot\nabla\right]\times$$
$$(\tilde{\varphi}(k;)J_0(k_{\perp}\varrho_{Lj}))$$
$$+O(\epsilon)$$

- Solution to the last eqn can be obtained by *Green function technique*: Replace the *r.h.s.* by a unit source. For a Sinusoidal time dependence, solve for the Green function or Propagator $\mathcal{P}$. An explicit analytical form is obtainable by the characteristics of unperturbed trajectories of the guiding centre and perturbation theory for velocity.

Global linear gyrokinetic theory (7)

- Note that for a unit source, $\mathcal{P}$ is only dependent on "equilibrium quantities"!
- This situation can be further simplified by choosing a simple distribution function, for example one without μ or pitch angle dependence.
- Assume for equilibrium f_{0j}, a local Maxwellian of the form

$$f_{0j}(\xi,\mu,\psi) = f_{Mj}(\xi,\psi) = \frac{N(\psi)}{\left(\frac{2\pi T_j(\psi)}{m_j}\right)^{3/2}} \exp\left(-\frac{\xi}{T_j(\psi)/m_j}\right)$$

  so that $\partial f_{0j}/\partial\mu \equiv 0$ by choice and density profile $N(\psi)$ is independent of the species type j.
- In terms of $\mathcal{P}$ solution to h_j^0 is in guiding center co-ordinates $\vec{R}$ is :

$$h_j^0(\vec{R},\vec{v},\omega) = -\left(\frac{q_j F_{Mj}}{T_j}\right)\int d\vec{k}\exp\left(\iota\vec{k}\cdot\vec{R}\right)\left(\omega-\omega_j^*\right)\left(\iota\,\mathcal{P}_j\right)\tilde{\varphi}(\vec{k};)J_0(k_\perp\varrho_{Lj}) + O(\epsilon$$

Global linear gyrokinetic theory (8)

- $\vec{k} = \kappa\ \hat{e}_\rho + k_\theta\ \hat{e}_\theta + k_\phi\ \hat{e}_\phi$ and $\kappa = (2\pi/\Delta\rho)\ k_\rho$, with $\Delta\rho = \rho_u - \rho_l$ which defines the radial domain, $k_\phi = n/r$ and $k_\theta = m/\rho$; ω is the $eigenvalue$ and $\omega_j^* = \omega_{nj}\left[1 + \frac{\eta_j}{2}\left(\frac{v_{||}^2}{v_{thj}^2} - 3\right) + \frac{\eta_j v_\perp^2}{2\ v_{thj}^2}\right]$ with $\omega_{nj} = (T_j \nabla_n \ln N k_\theta)/(q_j B)$ is the $diamagnetic\ drift\ frequency$; $\eta_j = (d\ln T_j)/(d\ln N)$.

- Note also that since the large aspect ratio equilibria considered are axi-symmetric, the toroidal mode number "n" can be fixed and the problem is effectively two dimensional in (ρ, θ) (configuration space) or (κ, k_θ) (Fourier space).

- To obtain the particle density fluctuation $\tilde{n}_j(\vec{r};\omega)$, one needs to go from guiding center $(g.c.)$ co-ordinate $\vec{R}$ to $particle\ co\text{-}ordinate\ \vec{r}$ using $\vec{R} = \vec{r} + \vec{v} \times \hat{e}_{||}/w_{cj}$, by replacing h_j using the adiabatic relationship discussed earlier, followed by the integration over $\vec{v}$ keeping in mind the $gyro\text{-}angle$ integration over α. This last integration on α yields an additional Bessel function "J_0" for $\tilde{\varphi}$, Thus, in real space $\vec{r}$, for species j, we finally have:

$$\tilde{n}_j(\vec{r};\omega) = -\left(\frac{q_j N}{T_j}\right)\left[\tilde{\varphi} + \int d\vec{k} \exp\left(\iota\vec{k}\cdot\vec{r}\right) \int d\vec{v} \frac{f_{Mj}}{N}\left(\omega - \omega_j^*\right)\left(\iota\mathcal{P}_j\right)\tilde{\varphi}(\vec{k};)J_0^2(x_{Lj}\right.$$

Global linear gyrokinetic theory (9)

- The solution $\mathcal{P}$ for a given $(\vec{k}, \omega)$ is simply

$$\mathcal{P}(\vec{R}, \vec{k}, \epsilon, \mu, \sigma, \omega) = \int_{-\infty}^{t} dt' \exp\left(\iota \left[\vec{k} \cdot (\vec{R}' - \vec{R}) - \omega t'\right]\right)$$
$$= \int_{-\infty}^{t} dt' \exp\left(\iota \int^{t'} dt'' \vec{k} \cdot \vec{v}_g(t'') - \iota\omega t'\right) \tag{9}$$

  where guiding center velocity $d\vec{R}/dt = \vec{v}_g = \vec{v}_{||} + \vec{v}_d$ and $\vec{R}(t)$ is to be obtained by solving for guiding center trajectories as an "initial value problem" in equilibrium considered above. This is done by first assuming that the cross-field drift terms $[\vec{v}_d]$ to be small and drop them at the zeroth order and to include them iteratively at the next order.

- This procedure gives us $\mathcal{P}$:

$$\iota\mathcal{P} = \sum_{p,p'} \frac{J_p(x_{tj}^{\sigma}) J_{p'}(x_{tj}^{\sigma})}{\omega - \sigma k_{||} v_{||} - p\omega_t} \exp(\iota(p - p')(\theta - \bar{\theta}_{\sigma})) \tag{10}$$

Global linear gyrokinetic theory (10)

- Here $x^{\sigma}_{tj} = k_{\perp}\xi_{\sigma}$, $\xi_{\sigma} = v_d/\omega_t, v_d = \left(v^2_{\perp}/2 + v^2_{||}\right)/(\omega_c R), \omega_t = \sigma v_{||}/(q(s)R), \sigma = \pm 1$ (sign of $\vec{v}_{||}$), $k_{\perp} = \sqrt{\kappa^2 + k^2_{\theta}}$, $k_{||} = [nq(s) - m]/(q(s)R)$ and $\bar{\theta}_{\sigma}$ is defined as $\tan\bar{\theta}_{\sigma} = -\kappa/k_{\theta}$ and $s = \rho/a$, $a-$is the minor radius.

- A few points to be noted here: (1) Note that the grad-B and curvature drift effects appear through the argument of Bessel functions ($x^{\sigma}_{tj} = k_{\perp}v_d/\omega_t$) of the Propagator. Thus for example, "radial and poloidal coupling" vanishes if $x^{\sigma}_{tj} = 0$ in for Propagator and one would arrive at "cylindrical" results. Hence in our model, Bessel functions in propagator bring about coupling between neighbouring flux surfaces and also couple neighbouring poloidal harmonics. (2) Argument of Bessel functions J_p's in Propagator solution is i.e., $x^{\sigma}_{tj} = k_{\perp}\xi_{\sigma}$ also depends on transit frequency ω_t, x^{σ}_{tj} can become $x_{tj} \simeq \mathcal{O}(1)$. Hence transit harmonic orders are to be chosen accordingly.

- In this form $\mathcal{P}$ contains effects such as transit harmonic and its coupling, parallel velocity resonances (Landau), poloidal mode coupling.

- Similar propagators can be constructed for trapped particles as well.

Global linear gyrokinetic theory (11)

- Quasineutrality condition yields the "closure".

$$\sum_j \tilde{n}_j(r;\omega) \simeq 0; \tag{11}$$

- Now, putting back the density fluctuations in the quasineutrality condition and fourier transforming yields a Convolution Matrix due to equilibrium inhomogeneity.

- $$\sum_{\vec{k}'} \sum_{j=i,e,f} \mathcal{M}^j_{\vec{k},\vec{k}'} \ \tilde{\varphi}_{\vec{k}'} = 0$$

  where $\vec{k} = (\kappa, m)$ and $\vec{k}' = (\kappa', m')$. Note that we could have 3 species: passing ions (i), passing electrons (e) and fast ions (f) or more. In the following we discuss in detail the formulation for passing species.

- Also, $\vec{k} = (\kappa, m)$ and $\vec{k}' = (\kappa', m')$. With the following definitions, $\Delta\rho = \rho_u - \rho_l$ (upper and lower radial limits), $\Delta_\kappa = \kappa - \kappa'$ and $\Delta_m = m - m'$ matrix elements are :

Global linear gyrokinetic theory (12)

- Matrix elements are :

$$\mathcal{M}^{i}_{\vec{k},\vec{k}'} = \frac{1}{\Delta\rho}\int_{\rho_l}^{\rho_u} d\rho \exp(-\iota\Delta_\kappa\rho) \times \left[\alpha_p\delta_{mm'} + \exp(\iota\Delta_m\bar{\theta})\sum_p \hat{I}^0_{p,i}\right]$$

$$\mathcal{M}^{e}_{\vec{k},\vec{k}'} = \frac{1}{\Delta\rho}\int_{\rho_l}^{\rho_u} d\rho \exp(-\iota\Delta_\kappa\rho) \times \left[\frac{\alpha_p}{\tau(\rho)}\delta_{mm'} + \frac{\exp(\iota\Delta_m\bar{\theta})}{\tau(\rho)}\sum_p \hat{I}^0_{p,e}\right] \quad (12)$$

$$\hat{I}^l_{p,j} = \frac{1}{\sqrt{2\pi}v^3_{th,j}(\rho)}\int_{-vmax_j(\rho)}^{vmax_j(\rho)} v^l_{||}dv_{||}\exp\left(-\frac{v^2_{||}}{v^2_{th,j}(\rho)}\right)\left\{\frac{N^j_1 I^\sigma_{0,j} - N^j_2 I^\sigma_{1,j}}{D^{\sigma,j}_1}\right\}_{p'=p-}$$

- Velocity Space Integrals are:

$$I^\sigma_{n,j} = \int_0^{v_{\perp max,j(\rho)}} v^{2n+1}_\perp dv_\perp \exp\left(-\frac{v^2_\perp}{2v^2_{th,j}(\rho)}\right) J^2_0(x_{Lj})J_p(x'^\sigma_{tj})J_{p'}(x'^\sigma_{tj})$$

Global linear gyrokinetic theory (13)

- The definitions for Vel. Integrals: $v_{\perp max,j(\rho)} = min(v_{||}/\sqrt{\epsilon}, v_{max,j})$ which is "trapped particle exclusion" from ω independent perpendicular velocity integral $I^{\sigma}_{n,j}$; $\alpha_p = 1 - \sqrt{\epsilon/(1+\epsilon)}$ is the fraction of passing particles; $\hat{I}^{l}_{p,j}$, is $\omega - dependent$ parallel integrals; $x^{\sigma}_{tj} = k_{\perp}\xi_{\sigma}$, $N^{j}_{1} = \omega - w_{n,j}\left[1 + (\eta_j/2)(v^2_{||}/v^2_{th,j}) - 3)\right]$; $N^{j}_{2} = w_{n,j}\eta_j/(2v^2_{th,j})$ and $D^{\sigma,j}_{1} =< w_{t,j}(\rho) > (nq_s - m'(1-p)(\sigma v_{||}/v_{th,j}) - \omega$ where $< w_{t,j}(\rho) >= v_{th,j}(\rho)/(rq_s)$ is the average $transit\ frequency$ of the species j.

- As integrals $I^{\sigma}_{n,j}$ are independent of ω and dependent only on $v_{\perp}$, σ and other equilibrium quantities, one may choose to calculate and store them as interpolation tables (memory intensive) or alternatively, one may choose to calculate them when needed (CPU-time intensive).

- Various numerical convergence tests should be performed with number of radial and poloidal Fourier modes, equilibrium profile discretization and velocity integrals.

Global linear gyrokinetic theory (14)

- Linear gyrokinetic eqns is formally solved using the equilibrium trajectories of particles.
- As the drift excursions are of $\mathcal{O}(\rho_{L,j}/R_0)$, a perturbative solution for guiding centre drift yields analytical solution for the Propagators (unit source solution) for both passing and trapped particles (not shown, but the method is the same!)
- This solution depends only on equilibrium quantities!
- Spatial inhomogeneity introduces coupling in spectral space $[\vec{k}]$.
- Model includes fully nonadiabatic ions, electrons and fast particles - all at the same physics footing!. This becomes possible because its a linear, spectral approach in space and time. Electrons and ions are not "pushed" in time.
- Particles which are deeply trapped or deeply passing are treated correctly. Model doesn't account for particles near the passing-trapping border in vel-space, as it is hard to obtain analytical equilibrium trajectories.

Global linear gyrokinetic theory (15)

- FLR effects to all orders in $k_\perp \rho_{L,j}$ are retained for all species!
- Shafranov shift and finite β effects are included, i.e. $(\varphi, A_{||}, A_\perp)$ fluctuations. Only electrostatic case without Shafranov shift was shown here.
- The model in its final form is solved numerically in the code EM-GLOGYSTO.
- Code is MPI based and runs on 15-20 nodes. Recently a portable version based on FFTW has been developed.
- Code was developed at Lausanne and later in India.